Available online at www.sciencedirect.com
ScienceDirect
Geochimica et Cosmochimica Acta 73 (2009) 2415–2440
Geochimica et Cosmochimica Acta
www.elsevier.com/locate/gca

Auger Nanoprobe analysis of presolar ferromagnesian silicate grains from primitive CR chondrites QUE 99177 and MET 00426

Christine Floss *, Frank Stadermann

Laboratory for Space Sciences and Physics Department, Washington University, One Brookings Drive, St. Louis, MO 63130, USA

Received 8 October 2008; accepted in revised form 12 January 2009; available online 20 February 2009

Abstract

We have investigated the presolar grain inventories of two CR chondrites, QUE 99177 and MET 00426, which are less altered than most members of this meteorite group. Both meteorites contain high abundances of O-anomalous presolar grains, with concentrations of 220 ± 40 and 160 ± 30 ppm for QUE 99177 and MET 00426, respectively. The presolar grain inventories are dominated by ferromagnesian silicates with group 1 oxygen isotopic compositions, indicative of origins in low mass red giant or asymptotic giant branch stars. Grains with pyroxene-like compositions are somewhat more common than those with olivine-like compositions, but most grains are non-stoichiometric with compositions intermediate between these two phases, consistent with recent work suggesting that amorphous interstellar silicates have stoichiometries between olivine and pyroxene type silicates. Although structural data are not available, one grain contains only Si and O, and has a stoichiometry consistent with SiO_2.

Our presolar grains are much more Fe-rich than predicted by astronomical observations. Although secondary alteration may play a role in enhancing the Fe contents of presolar grains, it seems unlikely that the large and ubiquitous Fe enrichments observed in the grains from this study can be due only to secondary processing, particularly given the highly primitive nature of these two meteorites. Grain condensation in the stellar outflows where these grains formed likely proceeded under rapidly changing kinetic conditions that may have enhanced the incorporation of Fe into the grains over that expected based on equilibrium condensation theory.

Both QUE 99177 and MET 00426 appear to contain unusually low abundances of oxide grains and have higher silicate/oxide ratios than other primitive meteorites analyzed to date. We explore various possibilities for this discrepancy, but note that most scenarios are not likely to result in the preferential destruction of oxides relative to silicates. Thus, the highest silicate/oxide ratios, such as those observed in the CR chondrites, should reflect the true initial proportions of presolar silicate and oxide grains in the parent molecular cloud from which the solar nebula evolved.

1. INTRODUCTION

Silicate grains are the newest addition to the collection of presolar minerals found in extraterrestrial materials. Initially discovered in interplanetary dust particles (Messenger et al., 2003a), they have since been found in a number of primitive meteorites (e.g., Mostefaoui and Hoppe, 2004; Nagashima et al., 2004; Nguyen and Zinner, 2004), and in Antarctic micrometeorites (Yada et al., 2008). Despite the relatively large numbers of presolar silicate grains found to date, there is still little information about the mineralogies and/or elemental compositions of most of them. Their small sizes (on the order of 200–500 nm) and the fact that they are generally embedded in matrices of abundant silicates of solar system origin, make the mineralogical identification of presolar silicate grains a non-trivial task. Spectroscopic observations of O-rich dust envelopes around evolved stars show the presence of both amorphous silicates and crystalline grains of forsterite, enstatite and diopside (Demyk et al., 2000). The few presolar silicates

* Corresponding author. Fax: +1 314 935 4083.
E-mail address: floss@wustl.edu (C. Floss).

0016-7037/$ - see front matter © 2009 Elsevier Ltd. All rights reserved.
doi:10.1016/j.gca.2009.01.033

characterized to date include crystalline olivine (Messenger et al., 2003a, 2005) and perovskite (Vollmer et al., 2007a) and non-stoichiometric amorphous phases (Nguyen et al., 2007; Vollmer et al., 2007b; Stroud et al., 2008), but also GEMS (glass with embedded metal and sulfides; Bradley, 1994), whose links to circumstellar environments are still ambiguous (Messenger et al., 2003a; Floss et al., 2006).

In addition, recent estimates (Floss et al., 2006; Nguyen et al., 2007) show that silicates may be the most common presolar phase (apart from nanodiamonds), with abundances that are up to one to two orders of magnitude greater than those of presolar SiC, graphite and oxide grains (Zinner, 2004). However, calculated abundances vary widely among different meteorites (e.g., Nagashima et al., 2004; Nguyen et al., 2007; Kobayashi et al., 2005) and it is not yet clear whether these differences are related to different degrees of thermal and/or aqueous alteration (e.g., Nagashima et al., 2005), heterogeneous distribution of presolar silicates in the chondrite forming regions of the solar nebula (e.g., Kobayashi et al., 2005), or simply limited sampling statistics or instrumental biases.

The CR chondrites, although they have experienced extensive aqueous alteration, are generally considered among the most primitive classes of meteorites (Krot et al., 2002) and contain insoluble organic matter (IOM) characterized as being primitive by various Raman parameters, frequently with H and N isotopic anomalies thought to be of interstellar origin (Busemann et al., 2006a, 2007), although a solar system origin has also been proposed for the D enrichments commonly observed (Remusat et al., 2006; Gourier et al., 2008). However, circumstellar silicate grains have only rarely been found in the CR chondrites studied to date (Nagashima et al., 2004; Floss and Stadermann, 2005), a fact that has been attributed to the aqueous alteration that they experienced. Abreu and Brearley (2006) recently reported the discovery of two CR chondrites, QUE 99177 and MET 00426, which are less extensively altered than most members of this group. We are investigating the circumstellar and interstellar grain inventories of these two meteorites in order to better understand the role that aqueous alteration plays in destroying presolar phases. Here we report on the isotopic compositions, mineralogies and distributions of O-anomalous circumstellar grains in QUE 99177 and MET 00426.

2. EXPERIMENTAL

We obtained one polished thin section each of QUE 99177 (26) and MET 00426 (24) from the Johnson Space Center Meteorite Curation Facility. The samples were initially documented using an Olympus BH-2 petrographic microscope to locate areas rich in matrix material for presolar grain searches.

Analyses to locate isotopically anomalous grains were carried out using the Washington University Cameca NanoSIMS 50 ion microprobe. We rastered a ~1-pA Cs^+ primary ion beam, with a diameter of ~100 nm, over individual matrix areas and collected secondary ions of $^{12}C^-$, $^{13}C^-$, $^{16}O^-$, $^{17}O^-$ and $^{18}O^-$, together with secondary electrons (SE). Sample areas of 12×12 μm^2 were pre-sputtered using a high beam current (~10 pA) to remove the carbon coat on the region of interest. Analyses then consisted of multiple scans (usually five) of 10×10 μm^2 (256^2 pixels) areas rastered within the pre-sputtered region that were added together to form one image measurement. Each analysis took approximately 2 h, with dwell times of 20,000 μs per pixel per scan. Mass peaks were automatically centered on $^{16}O^-$ after each scan and the positions of the masses on the other detectors were calibrated based on the shift in $^{16}O^-$. The analyses were carried out in automated mapping mode, with automatic stage movement to subsequent matrix areas, following a predefined grid pattern on the sample. The total areas of matrix material analyzed were 8500 μm^2 in QUE 99177 and 9200 μm^2 in MET 00426. Carbon and O isotopic compositions were normalized to the average composition of matrix material from each meteorite, assuming normal bulk isotopic compositions. Grains were considered presolar if their compositions deviated from the average surrounding material by more than 3σ and the anomaly was present in three consecutive image layers. Some grains sputtered away during the NanoSIMS analysis; this was usually obvious from the fact that the isotopic anomaly was no longer present in the final layer of the measurement. Additional details about the NanoSIMS analysis procedures and data reduction methods can be found in Stadermann et al. (2005).

Isotopically anomalous grains were analyzed for their elemental compositions using the Washington University PHI 700 Auger Nanoprobe. Following brief sputter cleaning with a widely defocused 2 kV 1 μA Ar^+ ion beam to remove atmospheric surface contamination, Auger electron energy spectra from 30 to 1730 eV were obtained with a 10-kV 0.25-nA primary electron beam with a diameter of 10–20 nm, which was rastered over areas of the grains of interest. Because the low beam current results in a low signal-to-noise ratio, multiple spectral scans of a given grain were subsequently added together to obtain a single Auger spectrum. These procedures were carried out in order to reduce the possibility of electron beam damage on these grains, which are often quite fragile; test measurements on standard grains have shown that high beam currents occasionally produce artifacts in the Auger spectra (Stadermann et al., in press). Auger spectra are typically differentiated using a 7-point smoothing and Savitsky–Golay differentiation routine prior to peak identification and quantification. Quantification was carried out using sensitivity factors for O (0.194), Si (0.121), Mg (0.234), Fe (0.150), Ca (0.626) and Al (0.160) obtained from a series of olivine and pyroxene standards with variable compositions (Stadermann et al., in press). These sensitivity factors have 1σ uncertainties of: O, 3.6%; Si, 11.0%; Fe, 11.2%; Mg, 9.4%; Ca, 10.8%; and Al, 24.9%. The high uncertainty for Al is due to the fact that Al is not very sensitive in the Auger Nanoprobe and the standards measured to date contain relatively low concentrations of this element. Not accounted for in the reported errors are various factors that can affect the quality of an Auger spectrum, including sample charging and the presence of surface contamination. We have also not corrected for background noise contributing to the spectra, which adds additional uncertainty, particu-

larly for elements present in low abundances. Thus, the errors reported here should be considered lower limits. High-resolution (10–20 nm) elemental distribution maps ($3 \times 3\ \mu m^2$ or $5 \times 5\ \mu m^2$; 256^2 pixels) of selected elements (e.g., O, Si, Fe, Mg, Ca, Al, S, and C) were also obtained for most grains after the quantitative measurements. Mapping was carried out at 10 kV with a 5-nA primary beam, and generally consisted of between 5 and 30 scans over the area of interest, depending on the element being mapped. These maps provide detailed qualitative information about the distribution of elements within and around the grains of interest, and may show the possible presence of rims and/or heterogeneities in the grains. Together with records of the size and location of the areas rastered during the spectral scans, they can also help identify extraneous contributions present in the Auger spectra that result from overlap of the raster area onto material surrounding the grain of interest. This can occur, for example, as the result of slight shifts of the beam during acquisition of the elemental spectra. Contaminating elements most commonly consisted of C and S, but in two cases (grain 6b-6-o1 from QUE 99177 and grain 4b-18-o1 from MET 00426) also included minor amounts of Fe, Mg and/or Si; these elements were not quantified for determining presolar grain compositions.

3. RESULTS

3.1. Isotopic compositions

From the C isotopic mapping we found numerous grains with anomalous C isotopic compositions in both QUE 99177 and MET 00426. These grains, as well as N isotopic measurements of both meteorites, will be the subject of a future paper. We note, however, that like other CR chondrites (e.g., Floss and Stadermann, 2005), QUE 99177 and MET 00426 do exhibit abundant and variable enrichments in ^{15}N (Floss and Stadermann, 2008a,b). Here we focus on the isotopic and elemental compositions of 61 grains with anomalous O isotopic compositions that we found in these two meteorites. Table 1 lists the isotopic compositions of the grains. Grains are identified by the matrix area in which they were measured (e.g., '5', '6b', and '2b'), followed by the specific raster ion image in that matrix area and finally by the grain number (e.g., 'o1' and 'o2'). In QUE 99177 31 of the 33 O-anomalous grains are ^{17}O-enriched with solar to slightly sub-solar $^{18}O/^{16}O$ ratios (Fig. 1). These grains belong to group 1, based on the classification system of Nittler et al. (1997). One grain from QUE 99177, 6-1-o1, is ^{18}O-rich and belongs to group 4 and the final grain, 6b-10-o2, is somewhat ^{18}O-rich for a group 1 grain and could also be classified as a group 4 grain. In MET 00426 most of the grains (23 of 28) also belong to group 1 (Fig. 1), and two additional grains show the ^{18}O enrichments of group 4 grains. Of the remaining three grains, one is depleted in ^{18}O with normal $^{17}O/^{16}O$, one is depleted in ^{17}O with slightly sub-solar $^{18}O/^{16}O$, and the third is enriched in ^{18}O and depleted in ^{17}O. The first two may be considered group 3 grains, whereas the composition of the latter falls between groups 3 and 4.

Table 1

Grain	Size (nm^2)	Group	$^{17}O/^{16}O$ ($\times 10^{-4}$)[a]	$^{18}O/^{16}O$ ($\times 10^{-3}$)[a]
(a) O isotopic compositions of presolar grains in QUE 99177				
5-4-o1	230 × 230	1	7.33 ± 0.32	1.92 ± 0.05
5-4-o2	190 × 190	1	7.00 ± 0.32	2.01 ± 0.05
5-7-o1	320 × 320	1	10.7 ± 0.3	1.84 ± 0.05
5-7-o2	350 × 350	1	6.86 ± 0.31	1.88 ± 0.05
5-7-o3	250 × 300	1	5.44 ± 0.26	1.85 ± 0.05
5-10-o11	200 × 150	1	7.52 ± 0.29	1.85 ± 0.05
5-11-o1	200 × 200	1	8.08 ± 0.39	2.00 ± 0.06
5-14-o1	230 × 230	1	5.91 ± 0.30	2.04 ± 0.06
5-15-o1	190 × 190	1	8.88 ± 0.34	1.87 ± 0.05
5-22-o1	250 × 300	1	8.92 ± 0.37	2.03 ± 0.05
5b-1-o1	230 × 230	1	18.3 ± 0.5	1.93 ± 0.05
5b-1-o2	190 × 190	1	17.6 ± 0.5	1.96 ± 0.05
5b-3-o1	300 × 300	1	13.0 ± 0.5	1.86 ± 0.06
5b-3-o2	250 × 250	1	7.80 ± 0.29	2.00 ± 0.05
5b-3-o3	190 × 190	1	6.00 ± 0.27	1.98 ± 0.05
5b-5-o1	150 × 150	1	4.78 ± 0.28	1.57 ± 0.05
5b-6-o1	230 × 230	1	5.77 ± 0.31	1.62 ± 0.05
5b-10-o1	230 × 260	1	6.96 ± 0.33	1.32 ± 0.04
5b-11-o1	230 × 230	1	5.39 ± 0.26	1.78 ± 0.05
5b-11-o2	230 × 230	1	5.25 ± 0.26	1.98 ± 0.05
6-1-o1	250 × 350	4	4.25 ± 0.24	3.77 ± 0.07
6-3-o1	230 × 230	1	5.90 ± 0.26	2.08 ± 0.05
6-8-o1	230 × 230	1	6.45 ± 0.34	1.39 ± 0.05
6b-2-o1	230 × 230	1	5.04 ± 0.21	2.12 ± 0.04
6b-6-o1	150 × 150	1	17.9 ± 0.4	1.99 ± 0.05
6b-10-o1	250 × 250	1	18.9 ± 0.5	1.95 ± 0.05
6b-10-o2	275 × 230	4?	5.97 ± 0.27	2.47 ± 0.06
6b-11-o1	230 × 310	1	8.00 ± 0.33	1.92 ± 0.05
7-1-o1	250 × 350	1	11.3 ± 0.3	1.83 ± 0.04
7-1-o2	300 × 250	1	5.74 ± 0.18	1.72 ± 0.04
7b-1-o1	190 × 230	1	6.27 ± 0.31	1.87 ± 0.05
7b-8-o1	190 × 190	1	5.99 ± 0.30	2.04 ± 0.05
8-5-o1	190 × 190	1	5.50 ± 0.27	2.01 ± 0.05
(b) O isotopic compositions of presolar grains in MET 00426				
2b-2-o1	*230 × 230*	*1*	*9.10 ± 0.29*	*1.87 ± 0.03*
2b-2-o2	*390 × 230*	*3*	*3.71 ± 0.14*	*1.47 ± 0.03*
2b-4-o1	230 × 230	3	2.52 ± 0.16	1.80 ± 0.04
2b-8-o1	250 × 300	1	8.10 ± 0.44	0.97 ± 0.05
2b-9-o1	230 × 230	1	5.21 ± 0.20	1.89 ± 0.04
2b-11-o1	230 × 230	1	6.90 ± 0.20	1.93 ± 0.03
2c-1-o1	*200 × 200*	*1*	*15.7 ± 0.4*	*1.79 ± 0.04*
2c-3-o1	200 x 200	1	4.94 ± 0.26	1.76 ± 0.04
2c-5-o1	190 × 190	1	10.2 ± 0.4	1.94 ± 0.05
2c-6-o1	*230 × 230*	*4*	*3.84 ± 0.22*	*2.92 ± 0.06*
2c-8-o1	*190 × 190*	*1*	*7.04 ± 0.35*	*1.94 ± 0.06*
2d-1-o1	190 × 190	1	5.05 ± 0.24	1.63 ± 0.04
2d-3-o1	300 × 300	1	5.99 ± 0.24	2.01 ± 0.04
2d-3-o2	250 × 250	1	5.74 ± 0.26	1.54 ± 0.04
4b-2-o1	230 × 230	1	5.55 ± 0.30	1.62 ± 0.05
4b-3-o1	190 × 190	1	6.78 ± 0.35	1.98 ± 0.06
4b-7-o1	190 × 190	1	7.21 ± 0.50	1.85 ± 0.08
4b-8-o1	190 × 250	1	6.07 ± 0.23	1.61 ± 0.04
4b-14-o1	250 × 200	1	5.94 ± 0.27	1.92 ± 0.05
4b-15-o1	*190 × 190*	*4?*	*3.03 ± 0.24*	*2.61 ± 0.07*
4b-17-o1	230 × 230	1	6.43 ± 0.37	1.12 ± 0.05
4b-18-o1	200 × 200	1	6.82 ± 0.35	1.91 ± 0.06
4b-20-o1	190 × 190	1	8.69 ± 0.12	1.04 ± 0.12
4c-2-o1	300 × 250	4	3.66 ± 0.27	3.03 ± 0.08
4c-3-o1	310 × 310	1	5.31 ± 0.30	1.75 ± 0.05

(*continued on next page*)

Table 1 (*continued*)

Grain	Size (nm^2)	Group	$^{17}O/^{16}O$ ($\times 10^{-4}$)[a]	$^{18}O/^{16}O$ ($\times 10^{-3}$)[a]
4c-7-o1	230 × 230	1	8.38 ± 0.57	1.97 ± 0.08
4c-12-o1	200 × 200	1	7.78 ± 0.34	1.77 ± 0.05
4c-18-o1	*190 × 190*	*1*	*5.99 ± 0.42*	*1.95 ± 0.07*

Grains in italics could not be measured for elemental compositions.
[a] Errors are 1σ.

3.2. Elemental compositions

We were able to use the Auger Nanoprobe to obtain compositional information for 54 of the 61 O-anomalous grains; of the remaining seven grains, all of them from MET 00426, four sputtered away during the NanoSIMS measurements and three could not be analyzed due to outgassing of a nearby alteration vein that deposited substantial C on the analysis regions. These grains are shown in italics in Table 1. Table 2 lists, for the grains that were analyzed, major element concentrations, Fe + Mg ± Ca/Si ratios, cation/O ratios, and possible phase identifications. Because we raster over predefined regions of the grains, the compositions in Table 2 are an average of the surface compositions (to a depth of a few nanometers, the extent sampled by the Auger electrons). As discussed in more detail below, some grains appear to be heterogeneous on a scale of 10s of nanometers, including in the third dimension. All but two of the presolar grains from QUE 99177 and MET 00426 appear to be ferromagnesian silicate grains. Several of these grains also contain Ca and/or Al. Notably, we only identified one oxide grain among the 54 O-anomalous grains for which we were able to determine compositions. The remaining grain appears to consist only of Si and O and is discussed separately.

Fig. 2 shows Fe + Mg ± Ca/Si ratios for the ferromagnesian silicate grains. Grains with olivine-like or pyroxene-like compositions can be distinguished on the basis of this ratio, with nominal values of 2 and 1, respectively. Fifteen grains have Fe + Mg ± Ca/Si ratios that (within 2σ errors) are consistent with pyroxene-like compositions and eleven grains have ratios that are consistent with olivine-like compositions (Table 2, Fig. 2). The remaining grains have non-stoichiometric compositions; these grains also do not have stoichiometries consistent with any other common silicate minerals. The Fe + Mg ± Ca/Si ratio does not take oxygen into account, which must also be present in stoichiometric proportions. This can be evaluated by comparing the cation/O ratios of the grains to the nominal values of 0.67 and 0.75 expected for pyroxene and olivine, respectively. From Table 2 it is evident that one grain (2d-1-o1 from MET 00426) identified as pyroxene on the basis of its Fe + Mg ± Ca/Si ratio has a cation/O ratio that is significantly higher than that expected for this mineral. Two grains with olivine-like compositions (5-22-o1 from QUE 99177 and 4c-2-o1 from MET 00426) likewise have cation/O ratios that are higher than expected. These grains have been flagged with question marks in Table 2 and Fig. 2. It is interesting to note, however, that no grains with pyroxene- or olivine-like compositions have low cation/O ratios that would indicate the presence of excess O, as has been observed in some GEMS from interplanetary dust particles (Bradley, 1994). In addition, although we sometimes observed the presence of S in some of our Auger spectra, elemental mapping of the areas around these grains showed that in all cases the S was present adjacent to the

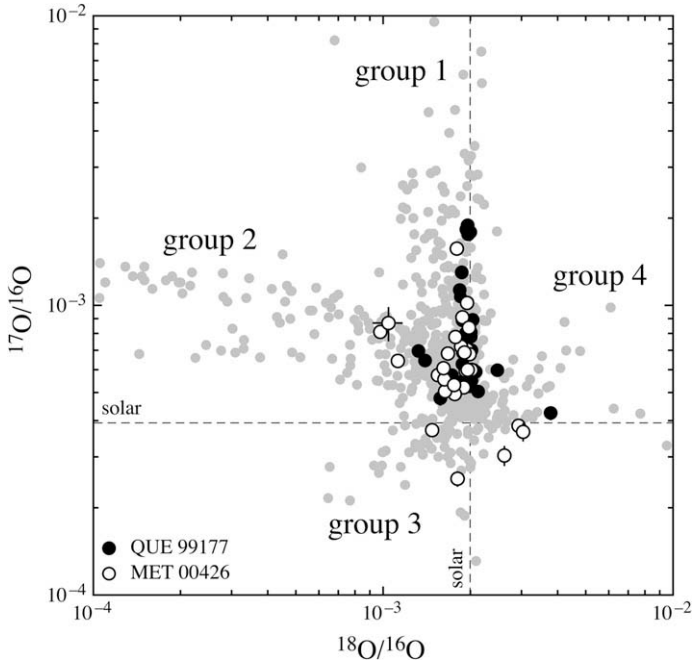

Fig. 1. Oxygen three isotope plot showing O-anomalous grains from QUE 99177 and MET 00426. Other data (gray circles) are from the literature (see Appendix A).

Table 2
(a) Major element concentrations (at.%) of presolar grains in QUE 99177[a]. (b) Major element concentrations (at.%) of presolar grains in MET 00426[a]

Grain	O	Si	Mg	Fe	Ca	Al	(Fe + Mg ± Ca)/Si	Cation/O	Mg#	Phase
QUE 99177										
5-10-o11	56.7 ± 2.0	21.9 ± 2.4	8.5 ± 0.8	12.9 ± 1.4			1.0 ± 0.1	0.76 ± 0.06	40	Pyroxene-like
5b-1-o2	61.1 ± 2.2	20.5 ± 2.3	9.8 ± 0.9	8.7 ± 1.0			0.9 ± 0.1	0.64 ± 0.05	53	Pyroxene-like
5b-11-o2	61.5 ± 2.2	17.7 ± 2.0	7.4 ± 0.7	13.3 ± 1.5			1.2 ± 0.2	0.62 ± 0.05	36	Pyroxene-like
6-3-o1	60.0 ± 2.2	18.9 ± 2.1	6.6 ± 0.6	14.5 ± 1.6			1.1 ± 0.2	0.67 ± 0.05	31	Pyroxene-like
6-8-o1	58.5 ± 2.1	22.4 ± 2.5	12.9 ± 1.2	6.3 ± 0.7			0.9 ± 0.1	0.71 ± 0.05	67	Pyroxene-like
6b-10-o1	62.4 ± 2.2	18.6 ± 2.0	13.9 ± 1.3	5.2 ± 0.6			1.0 ± 0.1	0.60 ± 0.05	73	Pyroxene-like
6b-11-o1	59.0 ± 2.1	21.6 ± 2.4	9.2 ± 0.9	10.2 ± 1.1			0.9 ± 0.1	0.70 ± 0.05	48	Pyroxene-like
5-7-o1	58.5 ± 2.1	13.7 ± 1.5	25.9 ± 2.4	1.9 ± 0.2			2.0 ± 0.3	0.71 ± 0.06	93	Olivine-like
5-7-o2	56.5 ± 2.0	13.8 ± 1.5	19.1 ± 1.8	10.6 ± 1.2			2.2 ± 0.3	0.77 ± 0.05	64	Olivine-like
5-22-o1	51.9 ± 1.9	15.0 ± 1.7	24.3 ± 2.3	8.8 ± 1.0			2.2 ± 0.3	0.93 ± 0.07	73	Olivine-like?
5b-5-o1	58.1 ± 2.1	12.8 ± 1.4	19.1 ± 1.8	10.1 ± 1.1			2.3 ± 0.3	0.72 ± 0.05	65	Olivine-like
6b-2-o1	55.5 ± 2.0	15.1 ± 1.7	16.7 ± 1.6	12.7 ± 1.4			1.9 ± 0.3	0.80 ± 0.06	57	Olivine-like
7-1-o1	57.6 ± 2.1	12.9 ± 1.4	24.5 ± 2.3	5.0 ± 0.6			2.3 ± 0.3	0.74 ± 0.05	83	Olivine-like
7-1-o2	57.1 ± 2.1	13.1 ± 1.4	24.8 ± 2.3	4.9 ± 0.6			2.3 ± 0.3	0.75 ± 0.06	84	Olivine-like
5-7-o3	58.9 ± 2.1	15.9 ± 1.7	12.8 ± 1.2	12.5 ± 1.4			1.6 ± 0.2	0.70 ± 0.05	51	Intermediate
5-11-o1	62.9 ± 2.3	14.7 ± 1.6	11.8 ± 1.1	10.6 ± 1.2			1.5 ± 0.2	0.59 ± 0.04	53	Intermediate
5-14-o1	60.1 ± 2.2	15.2 ± 1.7	6.9 ± 0.7	17.7 ± 2.0			1.6 ± 0.2	0.66 ± 0.05	28	Intermediate
5-15-o1	54.4 ± 2.0	19.1 ± 2.1	10.2 ± 1.0	16.4 ± 1.8			1.4 ± 0.2	0.84 ± 0.06	38	Intermediate
5b-1-o1	59.8 ± 2.2	15.2 ± 1.7	7.7 ± 0.7	17.3 ± 1.9			1.6 ± 0.2	0.67 ± 0.05	31	Intermediate
5b-3-o1	60.5 ± 2.2	17.5 ± 1.9	6.7 ± 0.6	15.3 ± 1.7			1.3 ± 0.2	0.65 ± 0.05	31	Intermediate
5b-3-o2	60.8 ± 2.2	15.4 ± 1.7	16.4 ± 1.5	5.0 ± 0.6	2.4 ± 0.3		1.6 ± 0.2	0.65 ± 0.05	77	Intermediate
5b-3-o3	57.2 ± 2.1	16.6 ± 1.8	8.9 ± 0.8	17.3 ± 1.9			1.6 ± 0.2	0.75 ± 0.06	34	Intermediate
5b-6-o1	59.0 ± 2.1	15.0 ± 1.7	18.2 ± 1.7	5.6 ± 0.6	2.1 ± 0.2		1.7 ± 0.2	0.69 ± 0.05	77	Intermediate
5b-10-o1	56.8 ± 2.0	16.5 ± 1.8	18.5 ± 1.7	8.2 ± 0.9			1.6 ± 0.2	0.76 ± 0.05	69	Intermediate
6b-10-o2	57.0 ± 2.1	18.3 ± 2.0	8.4 ± 0.8	16.3 ± 1.8			1.4 ± 0.2	0.75 ± 0.06	34	Intermediate
7b-8-o1	56.0 ± 2.0	18.0 ± 2.0	11.4 ± 1.1	14.5 ± 1.6			1.4 ± 0.2	0.78 ± 0.06	44	Intermediate
6-1-o1	59.6 ± 2.1	10.1 ± 1.1	25.9 ± 2.4	4.5 ± 0.5			3.0 ± 0.4	0.68 ± 0.05	85	Si-poor
5b-11-o1	52.0 ± 1.9	27.4 ± 3.0	5.4 ± 0.5	15.2 ± 1.7			0.8 ± 0.1	0.92 ± 0.08	26	Si-rich
7b-1-o1	43.7 ± 1.6	36.4 ± 4.0	5.1 ± 0.5	14.7 ± 1.6			0.5 ± 0.1	1.29 ± 0.11	26	Si-rich
8-5-o1	46.3 ± 1.7	29.8 ± 3.3		23.9 ± 2.7			0.8 ± 0.1	1.16 ± 0.10	0	Si-rich
5-4-o1	50.1. ± 1.8	12.9 ± 1.4	5.2 ± 0.5	19.7 ± 2.2		12.2 ± 3.0	1.9 ± 0.3	1.00 ± 0.09	21	Al-rich
5-4-o2	50.9 ± 1.8	12.8 ± 1.4	6.4 ± 0.6	20.2 ± 2.3	1.9 ± 0.2	7.7 ± 1.9	2.2 ± 0.3	0.96 ± 0.07	24	Al-rich
6b-6-o1	67.9 ± 2.4	32.1 ± 3.5						0.47 ± 0.05		SiO_2?

(*continued on next page*)

Table 2 (*continued*)

Grain	O	Si	Mg	Fe	Ca	Al	(Fe + Mg ± Ca)/Si	Cation/O	Mg#	Phase
MET 00426										
2b-9-o1	58.3 ± 2.1	21.8 ± 2.4	7.9 ± 0.7	11.9 ± 1.3			0.9 ± 0.1	0.71 ± 0.06	40	Pyroxene-like
2d-1-o1	53.3 ± 1.9	24.8 ± 2.7	5.8 ± 0.5	16.1 ± 1.8			0.9 ± 0.1	0.88 ± 0.07	27	Pyroxene-like?
2d-3-o1	57.3 ± 2.1	19.9 ± 2.2	9.8 ± 0.9	12.9 ± 1.4			1.1 ± 0.2	0.74 ± 0.06	43	Pyroxene-like
4b-2-o1	61.1 ± 2.2	17.3 ± 1.9	12.2 ± 1.1	9.4 ± 1.0			1.2 ± 0.2	0.64 ± 0.05	57	Pyroxene-like
4b-7-o1	59.1 ± 2.1	18.6 ± 2.0	9.7 ± 0.9	12.6 ± 1.4			1.2 ± 0.2	0.69 ± 0.05	43	Pyroxene-like
4b-20-o1	56.0 ± 2.0	23.5 ± 2.6	7.2 ± 0.7	13.4 ± 1.5			0.9 ± 0.1	0.78 ± 0.06	35	Pyroxene-like
4c-7-o1	60.0 ± 2.2	19.7 ± 2.2	6.7 ± 0.6	13.5 ± 1.5			1.0 ± 0.1	0.67 ± 0.05	33	Pyroxene-like
4c-12-o1	62.3 ± 2.2	19.7 ± 2.2	4.4 ± 0.4	10.5 ± 1.2	3.1 ± 0.3		0.9 ± 0.1	0.60 ± 0.05	29	Pyroxene-like
2b-8-o1	55.3 ± 2.0	15.3 ± 1.7	17.4 ± 1.6	12.0 ± 1.3			1.9 ± 0.3	0.81 ± 0.06	59	Olivine-like
2c-3-o1	56.5 ± 2.0	13.5 ± 1.5	22.3 ± 2.1	7.7 ± 0.9			2.2 ± 0.3	0.77 ± 0.06	74	Olivine-like
4c-2-o1	52.9 ± 1.9	14.9 ± 1.6	5.5 ± 0.5	26.7 ± 3.0			2.2 ± 0.3	0.89 ± 0.07	17	Olivine-like?
4c-3-o1	57.3 ± 2.1	13.8 ± 1.5	24.9 ± 2.3	4.1 ± 0.5			2.1 ± 0.3	0.74 ± 0.06	86	Olivine-like
2c-5-o1	58.8 ± 2.1	17.5 ± 1.9	7.4 ± 0.7	16.2 ± 1.8			1.3 ± 0.2	0.70 ± 0.05	32	Intermediate
2d-3-o2	59.1 ± 2.1	16.4 ± 1.8	14.4 ± 1.4	10.1 ± 1.1			1.5 ± 0.2	0.69 ± 0.05	59	Intermediate
4b-3-o1	53.6 ± 1.9	16.9 ± 1.9	6.9 ± 0.6	22.6 ± 2.5			1.7 ± 0.3	0.86 ± 0.07	23	Intermediate
4b-8-o1	56.4 ± 2.0	16.8 ± 1.8	13.3 ± 1.3	13.5 ± 1.5			1.6 ± 0.2	0.77 ± 0.06	50	Intermediate
2b-4-o1	56.6 ± 2.0	12.9 ± 1.4	21.3 ± 2.0	9.3 ± 1.0			2.4 ± 0.3	0.77 ± 0.05	70	Si-poor
2b-11-o1	56.2 ± 2.0	12.4 ± 1.4	20.7 ± 1.9	10.7 ± 1.2			2.5 ± 0.3	0.78 ± 0.06	66	Si-poor
4b-14-o1 (a)	56.3 ± 2.0	8.5 ± 0.9	27.4 ± 2.6	7.8 ± 0.9			4.1 ± 0.6	0.78 ± 0.06	78	Si-poor
4b-14-o1 (b)	53.1 ± 1.9	25.2 ± 2.8	12.2 ± 1.1	9.5 ± 1.1			0.9 ± 0.1	0.88 ± 0.07	56	
4b-17-o1	54.2 ± 2.0	26.5 ± 2.9	6.1 ± 0.6	12.0 ± 1.3	1.2 ± 0.1		0.7 ± 0.1	0.85 ± 0.07	34	Si-rich
4b-18-o1	57.9 ± 2.1					42.1 ± 10.5		0.73 ± 0.18		Al-oxide

[a] Errors are 1σ based on the uncertainties of silicate sensitivity factors; mg# = Mg/(Mg + Fe) * 100.

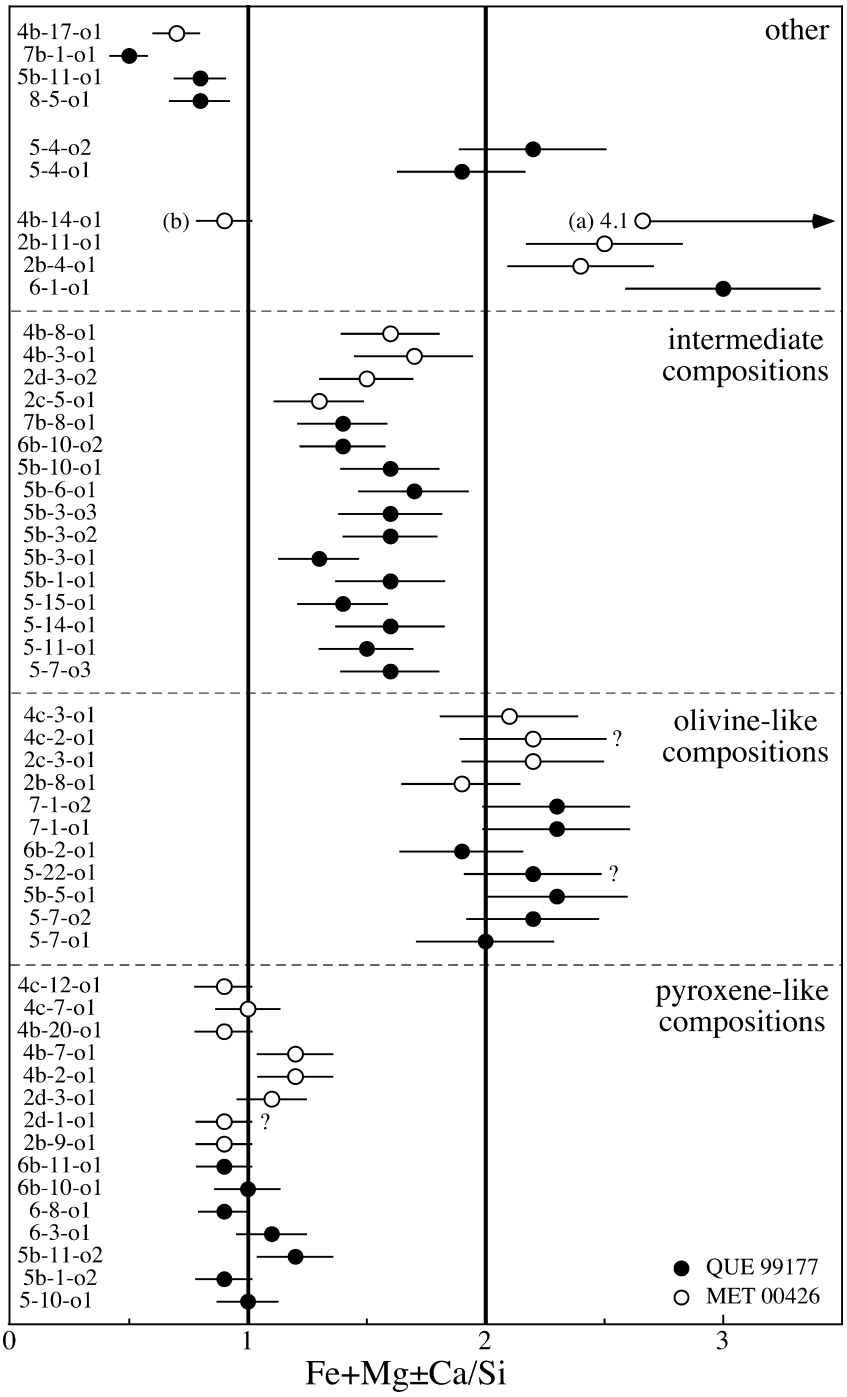

Fig. 2. Plot of Fe + Mg ± Ca/Si ratios in presolar ferromagnesian silicate grains from QUE 99177 and MET 00426. Errors are 1σ (Table 2). Question marks identify olivine-like or pyroxene-like grains with non-stoichiometric cation/O ratios. Two compositions are shown for grain 4b-14-o1. See text for details.

grain of interest, either as discrete grains or as a diffuse component of the surrounding matrix, but was not an intrinsic part of the grain itself, as would be expected in the case of GEMS. Fig. 3 shows field emission secondary electron (FE-SE) images of two grains with pyroxene-like compositions and two with olivine-like compositions; the Auger spectra for these grains are shown in Fig. 4. Grain 6-8-o1 (Fig. 3a) is a pyroxene-like grain from QUE 99177 that is about 230 nm in diameter, which is relatively Mg-rich (Fig. 4a). Grain 4c-12-o1 (Fig. 3b) from MET 00426 is also pyroxene-like and is about 200 nm across. This grain contains more Fe than Mg and is the only pyroxene-like grain that contains a substantial amount of Ca (Table 2 and Fig. 4b). Two olivine-like grains are shown in Fig. 3c and d. Grain 7-1-o2 (Fig. 3c) from QUE 99177 is about 300 × 250 nm in size and is Mg-rich (Fig. 4c), whereas grain

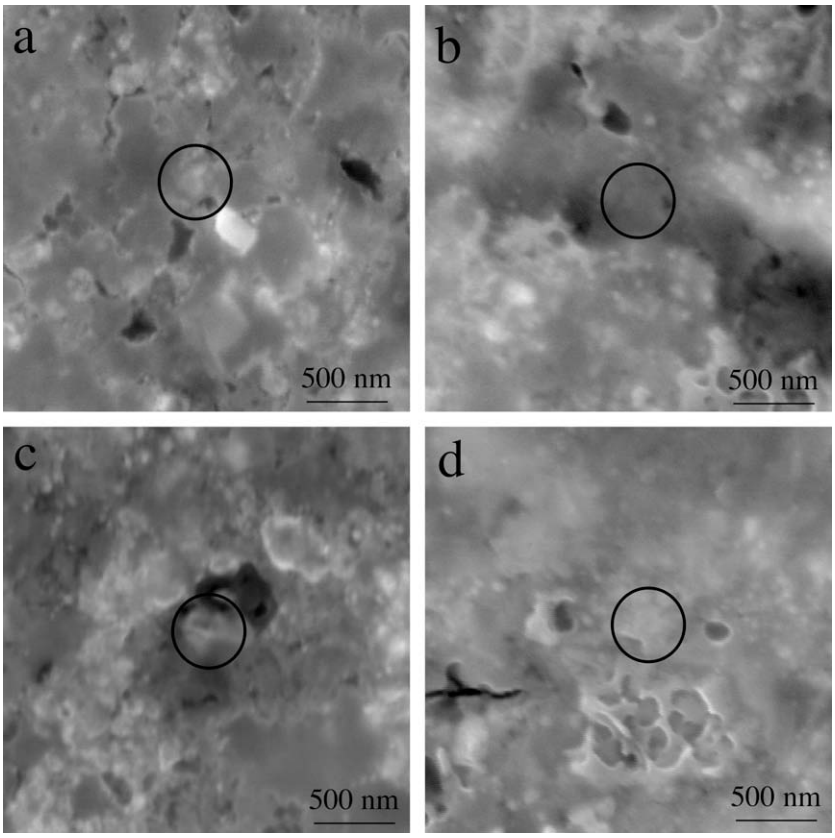

Fig. 3. Field emission secondary electron images of presolar grains with pyroxene-like (a and b) and olivine-like (c and d) compositions: (a) QUE 99177 grain 6-8-o1; (b) MET 00426 grain 4c-12-o1; (c) QUE 99177 grain 7-1-o2; and (d) MET 00426 grain 2b-8-o1.

2b-8-o1 (Fig 3d) from MET 00426 is similar in size, but contains more Fe (Fig. 4d). Overall there is a relatively large range in the Fe and Mg contents of the presolar grains (Table 2). Grains with pyroxene-like compositions have mg#s (atomic Mg/[Mg + Fe] * 100) from ~30 to 73, although most have more Fe than Mg (mg#s < 50). In contrast, grains with olivine-like compositions tend to be more Mg-rich, with mg#s from ~57 to 93. However one grain is very Fe-rich with an mg# of 17, although we note that it is one of two with cation/O ratios that are higher than expected for olivine.

Sixteen grains have Fe + Mg ± Ca/Si ratios that are intermediate (1.3–1.7) between pyroxene and olivine (Fig. 2) and have been labeled as intermediate in Table 2. Two of these grains also contain small amounts of Ca (Table 2). Quantification of the Auger spectra of over 100 standard olivine and pyroxene grains, using the procedures and sensitivity factors described above, resulted in Fe + Mg ± Ca/Si ratios for each mineral type with distributions that deviated from the nominal ratios in a roughly Gaussian manner (1σ standard deviations are 0.2 and 0.3 for pyroxene and olivine, respectively), with some overlap between the two populations at intermediate compositions (Stadermann et al., in press). Thus, some intermediate grains with non-stoichiometric compositions in terms of their Fe + Mg ± Ca/Si ratios may in fact belong to either the olivine-like or pyroxene-like groups. However, the number of these grains in our study is significantly larger than that expected from the Gaussian distribution observed in the standard grains, indicating that most of our intermediate grains do represent a distinct compositional group.

A number of grains do not fit into the scheme discussed above. Four grains are Si-poor with relatively high Mg contents (Table 2), leading to Fe + Mg ± Ca/Si ratios that are higher than those of olivine (Fig. 2). One of these is a relatively large (250 × 350 nm) group 4 grain from QUE 99177 that has an Fe + Mg ± Ca/Si ratio of 3 (Table 2). Fig. 5 shows the FE-SE image of grain 6-1-o1, along with Auger elemental maps showing the distributions of Mg, Fe and Si in this grain. Bose et al. (2008a) measured the Si isotopes in this grain and noted that although $^{30}Si/^{28}Si$ ratios are normal, there is a hint of a depletion in ^{29}Si at the 2σ level ($\delta^{29}Si = -58 \pm 28‰$; $\delta^{30}Si = -1 \pm 33$). Two of the other Si-poor grains, 2b-4-o1 and 2b-11-o1 from MET 00426, have Fe + Mg ± Ca/Si ratios that are only slightly higher than the ratio expected for olivine and cation/O ratios that are consistent with olivine. As discussed above, these compositions could be statistical outliers indicative of olivine-like grains. Finally, the remaining grain, 4b-14-o1 from MET 00426, is a bit enigmatic. Our initial analysis of this grain indicated a very Si-poor, Mg-rich composition with a Fe + Mg ± Ca/Si ratio of 4.1. However, Auger elemental distribution maps showed a heterogeneous distribution of Si in the grain and a subsequent quantitative analysis indi-

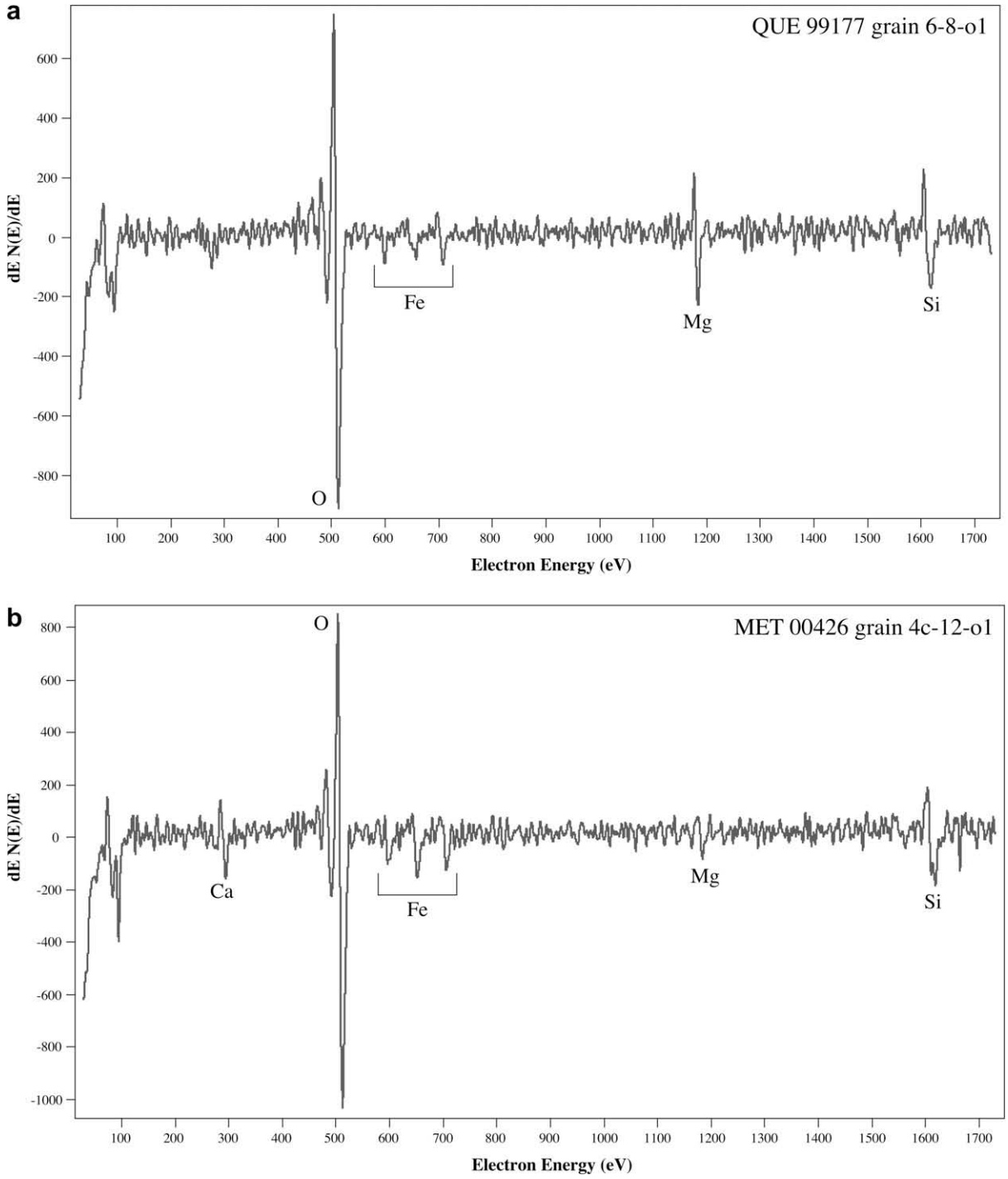

Fig. 4. Differentiated Auger elemental spectra for presolar grains with pyroxene-like compositions: (a) QUE 99177 grain 6-8-o1; (b) MET 00426 grain 4c-12-o1; (c) QUE 99177 grain 7-1-o2; and (d) MET 00426 grain 2b-8-o1.

cated a significantly more Si-rich composition and a Fe + Mg ± Ca/Si ratio consistent with pyroxene (Table 2 and Fig. 2). Although the observed heterogeneity (and concomitant analysis of a different portion of the grain) could account for some of the Si enrichment in the second analysis, it seems unlikely that this would result in a compositional shift of the magnitude observed. The origin of this discrepancy is unclear; we attempted to carry out a focused ion beam (FIB) extraction of the grain in order to clarify its composition, but the section was unfortunately lost during the process due to the presence of a sub-surface crack.

Another four grains, labeled Si-rich, exhibit elevated Si contents compared to olivine/pyroxene-like grains and have Fe + Mg ± Ca/Si ratios that are lower than those

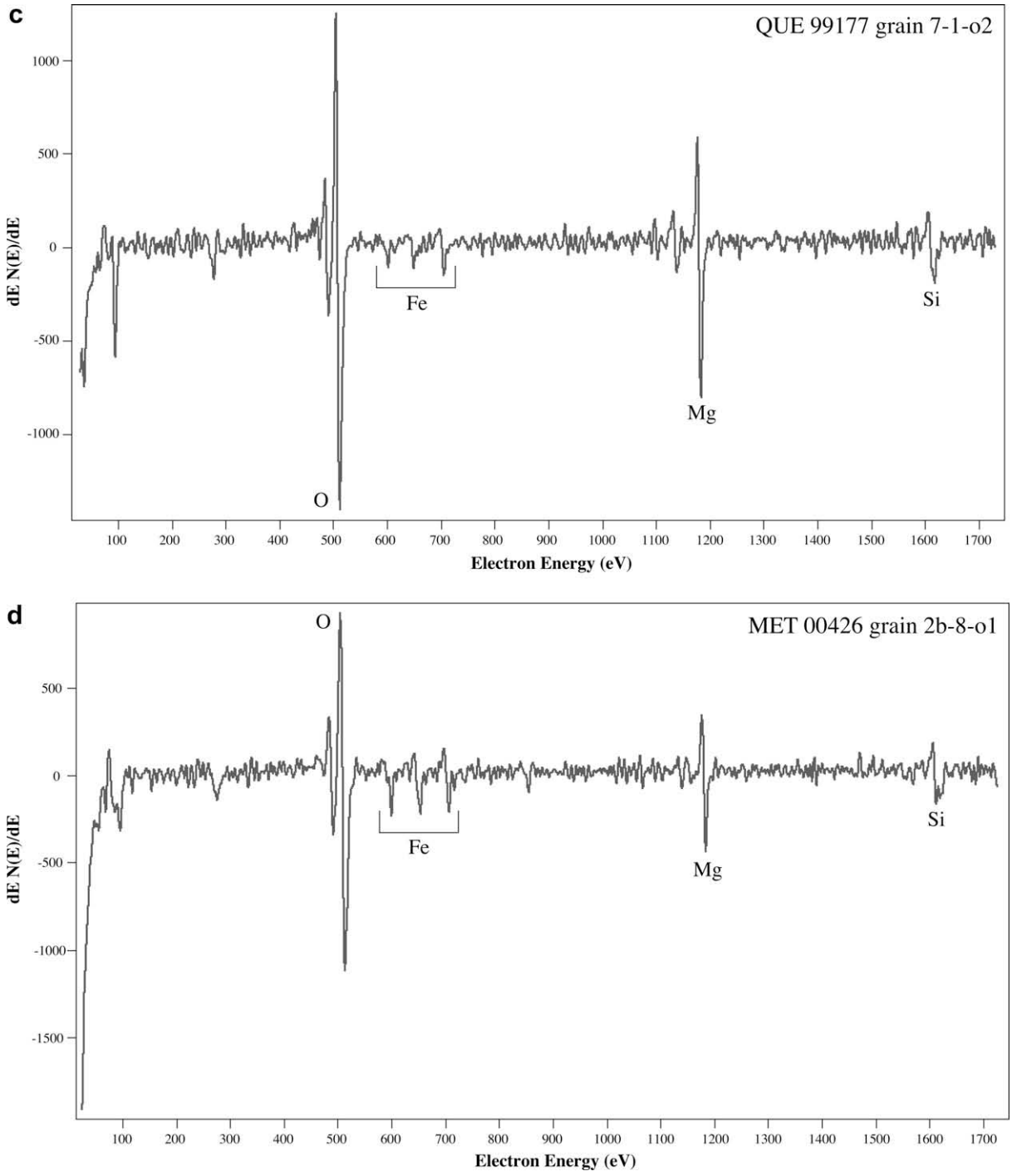

Fig. 4 (*continued*)

of pyroxene (Fig 2); all of these grains also contain more Fe than Mg, with one grain, 8-5-o1 from QUE 99177, containing no Mg at all (Table 2). One grain, 4b-17-o1 from MET 00426, also contains a small amount of Ca. Two additional non-stoichiometric ferromagnesian silicates are Al-bearing; one of them, grain 5-4-o2 from QUE 99177, also contains a small amount of Ca (Table 2). The Fe + Mg ± Ca/Si ratios of these grains are similar to those of olivine (Fig. 2) but the cation/O ratios of the grains are significantly higher than that expected for this mineral (Table 2). A third Al-rich grain, 4b-18-o1 from MET 00426, (Table 2) is a small oxide of about 200 nm in diameter that has a composition consistent with that of Al_2O_3. Finally, grain 6b-6-o1 from QUE 99177 appears to consist only of Si and O. This grain, shown in Fig. 6, is only about 150 nm in diameter. The Auger elemental

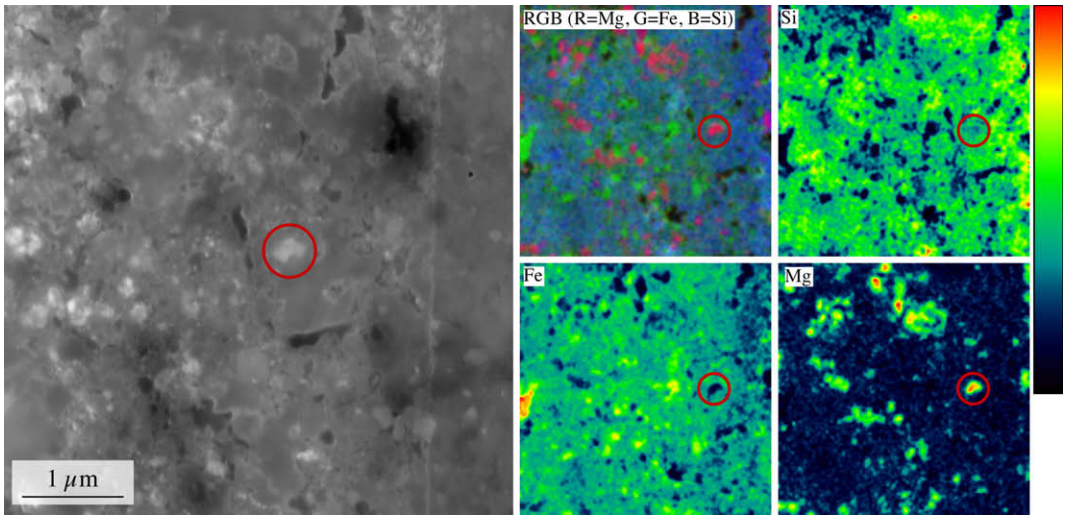

Fig. 5. Field emission secondary electron (left) and false color Auger elemental images (right) of presolar grain 6-1-o1 from QUE 99177. Note that the field of view for the SE image differs somewhat from that of the elemental images.

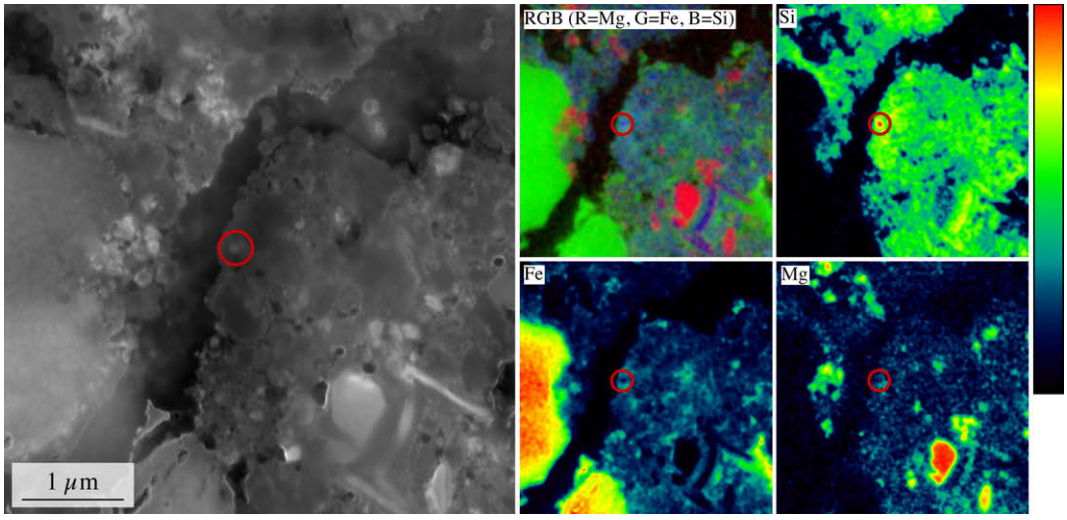

Fig. 6. Field emission secondary electron (left) and false color Auger elemental images (right) of presolar grain 6b-6-o1 from QUE 99177.

images show the strong enrichment in Si, and quantification of the Auger electron spectrum indicates that the grain has a Si/O ratio of ~0.5 (Table 2), suggesting that this grain may be SiO_2.

Two of the grains from this study, 4c-3-o1 and 2b-8-o1 both from MET 00426, were recently extracted using FIB and studied by TEM (Stroud et al., 2009); Auger data for both grains indicate olivine-like compositions (Table 2). The TEM results show that grain 4c-3-o1 has a mixed amorphous + finely nanocrystalline microstructure with SAED patterns for the crystalline portions that index to forsteritic olivine. EDX measurements show significant compositional heterogeneity within the grain, on a scale of 10s of nanometers. Grain 2b-8-o1 is more homogeneous, both in terms of structure and composition. It is also finely nanocrystalline with a composition that is in broad agreement with the Auger data.

4. DISCUSSION

4.1. Isotopic characteristics and stellar evolution

The overwhelming majority of the O-anomalous presolar grains in QUE 99177 and MET 00426, 54 of the 61, are group 1 grains. Another two grains belong to group 3, three grains belong to group 4, one grain is intermediate between groups 3 and 4, and one grain is intermediate between groups 1 and 4.

Presolar grains from groups 1 and 3, along with group 2 grains, are generally thought to have originated in oxygen-rich low-mass red giant and asymptotic giant branch (AGB) stars (e.g., Huss et al., 1994; Nittler et al., 1997). Nittler et al. (2008) have recently reviewed the evolution of low- and intermediate-mass stars ($<8\ M_{\odot}$). Briefly, hydrogen burning during the CNO cycles in the inner layers

of the star results in the production of ^{17}O and the destruction of ^{18}O (Boothroyd and Sackmann, 1999). As the star enters the red giant phase after H burning, this material is dredged up to the surface (the first dredge-up) of the star, resulting in enhanced $^{17}O/^{16}O$ and somewhat depleted $^{18}O/^{16}O$ ratios relative to the star's initial composition. After core He burning, the star enters the AGB phase, an active period involving thermal pulses and additional dredge-ups that are the major source of s-process elements (Busso et al., 1999), as well as extensive mass loss due to the strong stellar winds of these stars. Repeated dredge-up episodes eventually increase the C/O ratio until a carbon star forms. A final process of relevance to presolar oxide and silicate grains that occurs in low-mass AGB stars is 'cool bottom processing' (Wasserburg et al., 1995; Nollett et al., 2003): slow circulation of material from the star's envelope through hot regions near the H shell results in a decreased $^{18}O/^{16}O$ ratio relative to the initial composition of the star.

Fig. 7 shows the oxygen isotopic ratios expected for grains condensed from low-mass stars of initial solar metallicity. Also shown is the galactic chemical evolution line showing the expected evolution of oxygen isotopic ratios with increasing metallicity (Timmes et al., 1995). The bulk of the group 1 grains from QUE 99177 and MET 00426 are consistent with origins in low-mass (<2.0 $M_\odot$) red giant and AGB stars with metallicities that are fairly close to solar. However, several group 1 grains (three from MET 00426 and two from QUE 99177) have lower $^{18}O/^{16}O$ ratios ($<1.5 \times 10^{-3}$; Table 1) than most of the other group 1 grains (dashed circle in Fig. 7). Although these may have originated in lower metallicity stars than most of the group 1 grains, Nittler et al. (2008) suggested an alternative origin for such grains. Cool bottom processing, whereby ^{18}O is destroyed (Nollett et al., 2003), has commonly been invoked to account for the low $^{18}O/^{16}O$ ratios of the group 2 oxide and silicate grains. Nittler et al. (2008) showed that in addition to explaining the oxygen isotopic ratios of group 2 grains, cool bottom processing could also have affected the oxygen compositions of certain group 1 grains. Specifically they noted that the parent stars of group 1 grains with $^{18}O/^{16}O$ ratios of $<1.5 \times 10^{-3}$, such as those indicated in Fig. 7, could have started the AGB phase with oxygen compositions along the solar metallicity first dredge-up curve, as in Fig. 7, and had some ^{18}O subsequently destroyed by cool bottom processing (Nittler et al., 2008). One way to test whether cool bottom processing has affected the composition of a given grain is to determine its $^{26}Al/^{27}Al$ ratio, because ^{26}Al will also be produced in high amounts during this process (Nollett et al., 2003). Nittler et al. (2008) found that approximately 2/3 of their group 1 grains that were analyzed for Mg isotopes did contain evidence for ^{26}Al, whereas the remaining 1/3 did not. Thus, it appears that group 1 grains with low $^{18}O/^{16}O$ ratios can originate from both low metallicity stars as well as higher metallicity stars that have undergone cool bottom processing.

Another possibility is that these five grains are in fact group 2 grains whose oxygen isotopic compositions have been modified by contamination with isotopically normal oxygen from the surrounding matrix material due to beam overlap during the raster imaging analyses. Nguyen et al. (2007) modeled the effects of raster imaging analysis on the compositions of isotopically anomalous grains surrounded by isotopically normal grains and showed that strong dilution effects were observed among ^{18}O-depleted

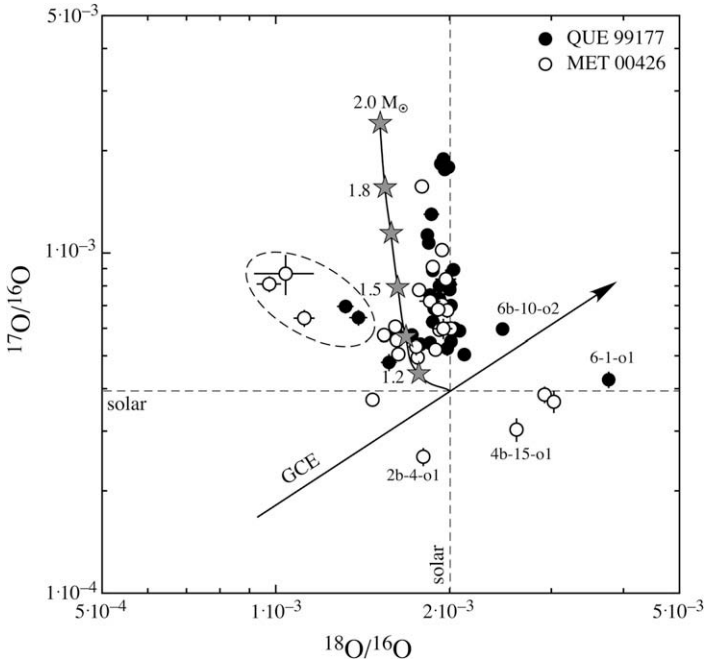

Fig. 7. Oxygen three isotope plot showing O-anomalous grains from QUE 99177 and MET 00426 together with models of the first and second dredge-up in low-mass red giant and AGB stars (Boothroyd and Sackmann, 1999). The arrow labeled 'GCE' indicates the expected galactic chemical evolution of oxygen isotopic ratios with increasing metallicity (Timmes et al., 1995).

group 2 grains, with dramatic shifts toward more normal $^{18}O/^{16}O$ ratios. Dilution effects are also grain-size dependent, with the largest shifts observed for the smallest grains. Simulation of the isotopic dilution of grains with typical group 2 compositions showed that grains in the size range of 150–250 nm might be expected to exhibit isotopic compositions similar to those observed for the five grains circled in Fig. 7 (see Fig. 3 of Nguyen et al., 2007). Thus, these grains, which have sizes ranging from 190–300 nm (Table 1), could, in fact, be group 2 grains whose isotopic compositions have been diluted with isotopically normal oxygen from surrounding material. However, as discussed at length by Nguyen et al. (2007), the variable factors influencing the degree of dilution preclude a determination of the original oxygen isotopic composition of any given grain.

Six grains have oxygen isotopic compositions that cannot be easily explained through origins in low mass red giant or AGB stars. Three of these, two from MET 00426 and one from QUE 99177, are group 4 grains (Table 1). One is a group 3 grain with a large depletion in ^{17}O, one is depleted in ^{17}O and enriched in ^{18}O and falls between groups 3 and 4, and the final grain is enriched in ^{17}O and ^{18}O and falls between groups 1 and 4.

The majority of group 4 grains identified to date define a linear trend with ^{17}O enrichments that are similar in magnitude to ^{18}O enrichments (Fig. 1; Appendix A). The origins of these grains have been quite enigmatic. Nittler et al. (1997) originally suggested that they might be produced either during early thermal pulses and third dredge-up events in AGB stars or in high metallicity red giant and/or AGB stars. However, both scenarios appear to be unlikely, the former because AGB models do not predict third dredge-up to occur during the earliest thermal pulses, and the latter because it would require much higher metallicities than would probably have been common at the time of formation of the solar system (Nittler et al., 2008). More recently, Nittler (2007) suggested that group 4 grains along this trend may have condensed in type II supernovae. Mixing calculations showed that the isotopic compositions of group 4 grains could be reproduced by mixing variable amounts of material from the inner ^{16}O-rich zones with a single mixture of the H envelope and the ^{18}O-rich He/C zone. The mixing line not only reproduces the group 4 oxygen data, but also passes near some ^{16}O-rich group 3 grains that are not well-explained by an AGB origin (Nittler, 2007). Nittler (2007) noted that not only did the results argue strongly for a supernova origin for most group 4 grains (and possibly some group 3 grains), but suggested that the narrow range of mixing conditions required to reproduce the grain data could indicate that the grains formed in a single supernova in which the mixing line may reflect a jet of ^{16}O-rich material from the inner part of the explosion passing through and mixing with the outer ejecta, followed by grain condensation (Nittler, 2007). Clearly such a scenario is speculative and would need to be corroborated with additional isotopic data, which is largely lacking for most group 4 grains at this point (e.g., Bose et al., 2008a). It is, however, consistent with the isotopic characteristics of grains such as 6b-10-o2 from QUE 99177, which is enriched in both ^{17}O and ^{18}O (Fig. 7). In addition, it could also account for grains such as group 3 grain 2b-4-o1 from MET 00426, which is depleted in ^{17}O (Fig. 7). The oxygen isotopic composition of this grain cannot be explained by dredge-up in a red giant or AGB star unless that star had an initial $^{17}O/^{18}O$ ratio much less than solar, since dredge-up will increase ^{17}O. However, this is not likely since the solar ratio is already lower than that of typical molecular clouds in the galaxy (Wilson and Rood, 1994). On the other hand, its isotopic composition does fall near the supernova mixing line calculated by Nittler (2007; see his Fig. 2).

Unlike most group 4 grains, however, the three group 4 grains from this study exhibit enrichments in ^{18}O, but have solar $^{17}O/^{16}O$ ratios and, thus, do not fall along the linear trend of correlated ^{17}O and ^{18}O enrichments discussed above. They are, in this respect, similar to two oxide and two silicate grains from earlier studies (Choi et al., 1998; Mostefaoui and Hoppe, 2004; Bland et al., 2007; Floss et al., 2008). Choi et al. (1998) were the first to propose a supernova origin for this type of grain. These authors noted that the high $^{18}O/^{16}O$ ratio and isotopic compositions of Mg, Ca and Ti of a corundum grain were compatible with formation in the ejecta of a 15-$M_\odot$ type II supernova. Similarly, Bland et al. (2007) argued for a supernova origin for a group 4 silicate with a large ^{18}O enrichment ($\sim 5\times$ solar) and a modest depletion in $\delta^{29}Si$ ($-96 \pm 27‰$). In contrast, Mostefaoui and Hoppe (2004) favored an AGB origin for an ^{18}O-rich pyroxene grain with modest enrichments in ^{29}Si and ^{54}Fe. These authors argued that the higher than solar O, Si and Fe ratios indicated an origin from a star with higher than solar metallicity, an argument that was challenged by Nittler et al. (2008), who noted that if this were the case, a much higher $^{17}O/^{16}O$ ratio would be expected, which is not observed. Finally, Floss et al. (2008) also argued for an AGB origin for an ^{18}O-rich magnesiowüstite grain. This grain exhibits only a modest enrichment in ^{18}O ($1.34\times$ solar) and shows depletions in both ^{54}Fe and ^{57}Fe. The isotopic constraints for this grain are ambiguous as current model predictions for both supernovae and AGB sources are inconsistent with the observed Fe isotopic compositions, whereas the modest ^{18}O enrichments could be accommodated by either stellar source. The authors ultimately favored an AGB origin based largely on astronomical evidence for the presence of magnesiowüstite in certain low mass-loss AGB stars (Floss et al., 2008).

Thus, it appears that no consensus has been found with regard to the origin of group 4 grains such as these, which exhibit enrichments in ^{18}O but have solar or close to solar $^{17}O/^{16}O$ ratios, and that few constraints can be placed on their stellar sources in the absence of isotopic data in addition to oxygen. We have additional isotopic information for only one of our grains in this category, grain 6-1-o1 from QUE 99177. As noted above, the Si isotopes for this grain suggest a slight depletion in ^{29}Si at the 2σ level, although the $^{30}Si/^{28}Si$ ratio is normal (Bose et al., 2008a). The enrichment in ^{18}O is relatively modest at 1.85 times the solar $^{18}O/^{16}O$ ratio. The enrichment in ^{18}O coupled with a depletion in ^{29}Si are qualitatively similar to the group 4 silicate studied by Bland et al. (2007) for which a supernova origin was suggested. Based on the 15-$M_\odot$ supernova model of

Rauscher et al. (2002), the bulk of this grain may have condensed from material from the outer zones and H envelope, which have O and Si compositions that are close to solar. The depletion in ^{29}Si can be produced by mixing a small amount (0.02%) of material from the inner Si/S zone, whereas ^{18}O is produced in the He/C zone; again only a small amount of material (~1%) is needed to account for the modest enrichment observed in the grain. Finally, one grain from MET 00426, 4b-15-o1, is depleted in ^{17}O but enriched in ^{18}O, falling between groups 3 and 4 (Fig. 7, Table 1). The oxygen isotopic composition of this grain is qualitatively similar to that of a supernova olivine grain from an anhydrous IDP reported by Messenger et al. (2005), although the magnitudes of the isotopic anomalies are significantly greater in the latter grain. Nevertheless, the similarity suggests that the grain from our study may also have a supernova origin.

4.2. Elemental compositions: observations versus expectations

4.2.1. Olivine-like, pyroxene-like and intermediate compositions

One of the most exciting results to come from the Infrared Space Observatory (ISO) is the discovery that, in addition to amorphous silicates, crystalline silicates are present around young main sequence stars (Waelkens et al., 1996; Malfait et al., 1998) and oxygen-rich AGB stars (Waters et al., 1996; Demyk et al., 2000). The majority of the features in the spectra can be explained by crystalline forsterite and enstatite, with enstatite about 3–4 times more abundant than forsterite for most stellar sources (Molster et al., 2002a); the presence of crystalline diopside has also been proposed (Demyk et al., 2000). Although the broad features of amorphous silicates allow a less detailed analysis, they indicate primarily olivine compositions, with pyroxene compositions probably representing less than 10% of the total amorphous silicate mass (Demyk et al., 2000). The dust in most stellar sources is dominated by amorphous silicates, although stars with up to 75% crystalline silicates have been observed (Molster et al., 2001). Auger spectroscopy, just like EDX and electron microprobe analysis, does not provide structural information about phases and, therefore, we do not know whether the majority of our presolar grains are crystalline or amorphous. Indeed, as noted above, TEM data for one of the two grains from this study that have been FIB-extracted indicate that both amorphous and nanoscale crystalline domains can be present within single grains (Stroud et al., 2009). In our study grains with pyroxene-like compositions tend to be somewhat more common than those with olivine-like compositions, although within 1σ errors the numbers are not statistically different; nine grains have compositions consistent with olivine and fourteen have compositions consistent with pyroxene (these numbers do not include those grains in which the cation/O ratios are not stoichiometric). The distribution of our grains is, thus, not consistent with that expected from either predominantly crystalline or predominantly amorphous sources, from which one would expect primarily pyroxene or olivine compositions, respectively. Rather, if grain compositions can be used as a guide to the type of source, the distribution suggests that both crystalline and amorphous sources contributed to the presolar grain population present in these two meteorites. In addition, a large fraction of the presolar silicate grains that we observe in our population have compositions that are intermediate between those of olivine and pyroxene (Table 2 and Fig. 2). A recent study by Min et al. (2007) suggests that amorphous silicates in the interstellar medium are expected to have a stoichiometry in between that of olivine and pyroxene type silicates, with an O/Si ratio of ~3.5, identical to the average O/Si ratio of our intermediate type grains. However, Min et al. (2007) also predict highly magnesian compositions, in contrast to the relatively Fe-rich nature of our grains (see below).

4.2.2. Si-rich and Si-poor grains

Four grains have elevated Si abundances with low Mg/Fe ratios; one grain contains no Mg at all (Table 2). One of these grains, 4b-17-o1 from MET 00426, also contains a small amount of Ca. These Si-rich grains all have Fe + Mg ± Ca/Si ratios lower than those of pyroxene (Fig. 2), elevated cation/O ratios compared to either olivine or pyroxene and have mg#s that are among the lowest in our population of presolar silicate grains. Nagahara and Ozawa (2008) have suggested that Si enrichment can occur in the gas phase through heterogeneous nucleation of Fe metal onto forsterite, which inhibits the standard equilibrium reaction of forsterite with gas to form enstatite, and ultimately leads to the non-equilibrium condensation of Si-enriched phases such as SiO_2. As these authors note, the actual reactions that take place in the stellar environments are likely to fall between the equilibrium and kinetic extremes and the products produced may be mixtures of these endmember phases. Indeed, the condensation of metastable Fe- and/or Si-rich phases has been demonstrated experimentally in laboratory smokes (Rietmeijer et al., 1999; Nuth et al., 2000). Enhanced SiO emissions have also been observed in high velocity protostellar molecular outflows where production of SiO is mainly due to the shock processing of dust at high temperatures (Nisini et al., 2002). Subsequent condensation may result in Si-enriched grains (e.g., Aléon et al., 2005). Grains enriched in Si may also condense from gases with low Mg/Si ratios, as discussed below for the formation of SiO_2 (Ferrarotti and Gail, 2001). Stars with low Mg/Si ratios are expected to make up approximately 10% of the total stellar population. All four of the Si-rich grains have group 1 oxygen isotopic compositions. One of them (4b-17-o1 from MET 00426) is one of five grains with lower ^{18}O/^{16}O ratios than most of the other group 1 grains (Fig. 7). As discussed above, such grains can originate from low metallicity stars or from stars with higher metallicity that have experienced cool bottom processing. Low Mg/Si abundance ratios in stars seem to be coupled to lower-than-solar metallicities (Ferrarotti and Gail, 2001), suggesting that formation of grain 4b-17-o1 in a low metallicity star with a low Mg/Si ratio may be more likely than an origin involving cool bottom processing.

Four stardust grains have Fe + Mg ± Ca/Si ratios that are higher than those of olivine, ranging from 2.4 to 4.1 (Tables 2a and b, and Fig. 2). As noted earlier, the elevated ratios of these grains are the result of low Si contents compared with olivine-like grains, rather than higher Mg or Fe contents; all of the grains also have high mg#s. As discussed above, the Auger results from grain 4b-14-o1 from MET 00426 are inconsistent, and, thus, this grain is not discussed further here. Two of the grains, 2b-4-o1 and 2b-11-o1 from MET 00426, have Fe + Mg ± Ca/Si ratios that are only slightly higher than those of olivine and these grains could therefore belong to the population of olivine-like grains, as noted earlier. Grain 6-1-o1 from QUE 99177, however, has a Fe + Mg ± Ca/Si ratio of 3.0 (Table 2) and a non-stoichiometric composition that is intermediate between that of olivine and magnesiowüstite, the solid solution series consisting of endmembers periclase (MgO) and wüstite (FeO). Calculations by Gail and Sedlmayr (1999) and Ferrarotti and Gail (2001) suggest that periclase or MgO can form under non-equilibrium conditions in stellar outflows, particularly at high Mg/Si ratios. Ferrarotti and Gail (2003) explored in more detail the formation conditions of magnesiowüstite. Their results show that magnesiowüstite is a likely condensate in the stellar outflows of oxygen-rich AGB stars with low mass-loss rates ($M \leqslant 4 \times 10^{-6}$ $M_{\odot}$ year^{-1}). At higher mass-loss rates the condensation of magnesiowüstite is suppressed by the early condensation of silicates, and olivine will be the first phase to form. Laboratory studies of silicate smokes have also demonstrated the kinetic formation of non-stoichiometric Mg endmember oxide and silicate phases (e.g., Nuth et al., 2000). Thus, grains such as 6-1-o1, and possibly also 2b-4-o1 and 2b-11-o1, may form metastably as non-stoichiometric mixtures of Mg-rich oxide and silicate phases in the rapidly changing stellar environment. Another possibility is that we are measuring grains with heterogeneous structures and/or compositional regions, because we are rastering over the entire surface areas of the grains and thereby obtaining averaged compositional information. Grains with internal heterogeneities have been found among the presolar silicate population through FIB/TEM analysis (Vollmer et al., 2007b; Stroud et al., 2008, 2009) and may also form in the rapidly cooling environments of stellar outflows. The Si-poor grains in our population do not originate from a single stellar source. One of them, 2b-11-o1 from MET00426, is a group 1 grain, with an origin in a low mass AGB or red giant star, the second grain, 2b-4-o1 from MET 00426, is the ^{17}O-depleted group 3 grain whose oxygen isotopic composition falls along the supernova mixing line of Nittler (2007) as noted above, and the final grain, 6-1-o1 from QUE 99177, is a group 4 grain, discussed earlier, for which a supernova origin is advocated on the basis of its Si isotopic composition.

4.2.3. Al-rich grains

Three grains have detectable amounts of Al and are listed separately in Table 2. One of these, 4b-18-o1 from MET 00426, is an Al-oxide grain with a stoichiometry consistent with that of Al_2O_3 (Table 2). The other two grains are Al-bearing ferromagnesian silicates, one of which, 5-4-o2 from QUE 99177, also contains a small amount of Ca. If we assume a pyroxene stoichiometry for these two grains and add the Al component to that of Si, the calculated Fe + Mg ± Ca/Si + Al ratios would change from 1.9 to 1.0 for 5-4-o1 and from 2.2 to 1.4 for 5-4-o2, suggesting a pyroxene-like composition for the former grain; however, its cation/O ratio is significantly higher than that of pyroxene. The presence of abundant Al in these grains indicates a more refractory component than is present in the other ferromagnesian silicates. Recent findings indicate the presence of abundant Al-bearing phases in O-rich evolved stars, particularly in the early AGB phase when mass-loss rates are low (e.g., Speck et al., 2000; Sloan et al., 2003; DePew et al., 2006; Maldoni et al., 2008). Al_2O_3 is expected to be the first solid to condense from an O-rich circumstellar gas (Lodders and Fegley, 1999) and is well-known from the presolar grain inventory of primitive meteorites (e.g., Nittler et al., 1994, 1997, 2008). As temperatures decrease, Al_2O_3 can act as a nucleation site for the subsequent condensation of ferromagnesian silicates (e.g., Gail and Sedlmayr, 1999; Demyk et al., 2000; Toppani et al., 2006) or can react with the gas to form other Al-bearing silicates such as gehlenite. Auger elemental maps of the two Al-bearing silicate grains in our presolar grain inventory do not show any zoning patterns or core enrichments of Al indicating that these grains do not represent seed nuclei upon which other phases have condensed. However, Vollmer et al. (2006) identified a relatively large (~1 μm) presolar silicate from Acfer 094 that appeared to consist of an Al-rich center surrounded by a Si-rich rim, although attempts to extract the grain with FIB were unsuccessful and no additional information could be obtained. The presence or absence of such core grains can provide important constraints on the stellar environments in which presolar silicates formed. Calculations by Sogawa and Kozasa (1999) suggest that at high mass-loss rates crystalline silicates can form around previously condensed Al_2O_3 cores, whereas homogeneous grains remain amorphous. The Al-bearing silicate grains from our study do not have compositions consistent with any stoichiometric mineral phases. Like the Si-rich and Si-poor grains discussed above, they may be the products of kinetic processes taking place in a rapidly changing stellar environment. All three of the Al-bearing grains (silicates 5-4-o1 and 5-4-o2 from QUE 99177, and oxide 4b-18-o1 from MET 00426) belong to group 1 and have similar oxygen isotopic compositions (Table 1).

4.2.4. SiO_2 grain

SiO_2 has been predicted to form in the outflows of oxygen-rich stars during rapid cooling under non-equilibrium conditions in stars with low Mg/Si ratios (Gail and Sedlmayr, 1999; Ferrarotti and Gail, 2001). Calculations by Ferrarotti and Gail (2001) suggest that for Mg/Si ratios <1 the amount of silica produced is expected to be sufficient to allow detection of this phase as a distinct component in stars with low Mg/Si abundance ratios. Indeed, although forsterite and enstatite have been able to account for many of the features seen in the spectra of evolved oxygen-rich stars, other phases, including SiO_2, have been suggested as potential sources to account for as yet unidentified features in

these spectra (Molster et al., 2002b; Molster and Waters, 2003). Specifically, Molster et al. (2002b) suggested that the sharp band at 20.5 μm could be attributed to silica, although they noted that the width of the feature was considerably narrower than laboratory spectra of silica, a feature they suggested could be due to temperature effects. As noted earlier, one of the grains found in QUE 99177, 6b-6-o1, appears to consist only of Si and O and has a stoichiometry consistent with SiO_2 (Table 2 and Fig. 6). We note, moreover, that measurement of a quartz standard showed that the sensitivity factors obtained from our olivine and pyroxene standards are valid for SiO_2 as well. The grain is a group 1 grain and has one of the most ^{17}O-rich compositions measured in this dataset (Table 1). The grain is very small (~150 nm) and its Auger spectrum contains minor amounts of C, Fe and Mg in addition to O and Si. However, as discussed above, (see Section 2), based on the Auger elemental mapping and the size and location of the raster area used to obtain the Auger spectrum, these elements appear to be contaminants that originate from areas adjacent to the grain and, thus, are not indigenous to the grain's composition. Unfortunately, because of the small size of the grain, it is not a good candidate for FIB extraction. Although our identification of this grain as SiO_2 is not absolutely certain, and we do not have structural data to confirm its crystallinity, the highly Si-enriched composition of the grain does provide strong indication that phases similar to silica are present in the presolar grain population. Amorphous silica grains with extreme oxygen isotopic anomalies have also been reported from the Murchison CM chondrite (Aléon et al., 2005). The grains, which were found within insoluble organic matter isolated from the meteorite, have correlated ^{17}O and ^{18}O excesses consistent with a single isotopically heavy oxygen reservoir, and Si isotopes that are consistent with terrestrial values. In this case, the authors have argued for a solar system origin for these grains, with production of the oxygen isotopic anomalies through irradiation from impulsive solar flares (Aléon et al., 2005).

4.2.5. TEM observations

Presolar silicate grains analyzed to date by TEM include GEMS grains (Floss et al., 2006; Messenger et al., 2003a), crystalline olivine grains (Messenger et al., 2003a, 2005), a crystalline MgSi perovskite grain (Vollmer et al., 2007a), as well as several amorphous and/or inhomogeneous glassy grains or aggregates (Nguyen et al., 2007; Stroud et al., 2008; Vollmer et al., 2007b). One of the two grains from this study extracted for TEM analysis, 4c-3-o1 from MET 00426, is also compositionally and structurally heterogeneous, with amorphous domains as well as nanocrystalline domains of forsteritic olivine. The other grain, 2b-8-o1 from MET 00426, is more uniform, with a compositionally homogeneous finely nanocrystalline structure (Stroud et al., 2009). Notably absent thus far from the TEM data are any crystalline or amorphous grains with pyroxene compositions, although a relatively large number of such grains are present in our study. We should note, moreover, in this context that both the cation/O and Fe + Mg ± Ca/Si ratios for pyroxene would be equally consistent with the MgSi perovskite identified by Vollmer et al. (2007a), and that structural information is required to distinguish between the two possibilities. Perovskite is a high-pressure phase that is not predicted to form by equilibrium condensation in low-pressure stellar environments. Vollmer et al. (2007a) propose several possible formation scenarios, including shock transformation and a chemical vapor deposition-like process to account for the origin of this grain. However, some of these processes are rather speculative and it seems unlikely that high-pressure perovskite can account for all of the pyroxene-like compositions observed in this study. Pyroxene-like compositions can also be produced by low energy irradiation (Demyk et al., 2001). These authors noted that irradiation of crystalline olivine with low energy He^+ ions not only amorphized the olivine grains, but reduced the O/Si and Mg/Si ratios of the irradiated layers toward pyroxene-like compositions. They concluded that irradiation of interstellar silicate grains in supernova shocks is probably responsible not only for the lack of crystalline silicates in the interstellar medium, but also for the observed evolution of silicates from olivine-type grains around AGB stars to pyroxene-type grains around protostars (Demyk et al., 2001). Such an explanation is consistent with our observation of more grains with pyroxene-like compositions than olivine-like compositions.

Another difference between the TEM data and the grains from our study is the lack of any GEMS in our presolar grain population. One possible explanation for this is that we simply cannot identify GEMS grains accurately on the basis of Auger elemental compositions. This seems unlikely as the Auger technique is quite sensitive for the S we would expect to see from the embedded sulfides; indeed as noted earlier, we found S contamination in several spectra from adjacent matrix material. Moreover, SE images of the grains should provide some clue to the possible presence of GEMS; we note that Floss et al. (2006) initially identified as GEMS a presolar grain in the IDP Eliot, on the basis of its appearance in an SE image, an identification that was later confirmed by TEM examination of a FIB extracted section of the grain. Thus, the absence of any possible GEMS candidates in our study appears to be real and is probably not an artifact of the analytical tools available to us. The apparent lack of GEMS in our study relates to a more general question about the distribution of GEMS in extraterrestrial matter. Although virtually all GEMS identified to date have been found in IDPs, Noguchi et al. (2008) recently made the first positive identification of GEMS grains in Antarctic micrometeorites, although it is not clear if these grains are isotopically anomalous or not. However, GEMS have not yet been unambiguously identified from any primitive meteorites. Given the uncertainty over how GEMS originated and whether they are predominantly solar or presolar in origin (e.g., Bradley and Dai, 2004; Keller and Messenger, 2004), it is of importance to clarify whether the apparent absence of GEMS from primitive meteorites is real or not. This may require a concerted effort to locate such grains, not necessarily among presolar silicate grains but in the matrix material of suitable primitive meteorites, such as QUE 99177 and MET 00426.

The presolar silicate population is obviously complex and much additional work will be required to identify the variety of phases present, and to correlate these observations with those made spectroscopically around oxygen-rich stars and in the interstellar medium.

4.3. Iron abundances in silicate stardust grains

The crystalline phases expected to be present in stellar outflows are the Mg-rich endmembers of olivine and pyroxene, with the amount of Fe constrained to be less than 10% (Demyk et al., 2000). Amorphous grains, in contrast, have generally been expected to be more Fe-rich than crystalline silicates based on their higher absorptivity in the near-infrared (Molster et al., 1999, 2002a; Demyk et al., 2000; Kemper et al., 2004). However, Min et al. (2007) recently investigated the composition and shape distribution of interstellar silicate dust grains using realistic particle shapes rather than the homogeneous spheres commonly used in past studies. Among other results, their modeling suggested that amorphous silicates in the interstellar medium in fact are highly magnesium-rich, with mg#s >90. They, along with others, have argued that Fe must instead be present the form of phases such as metallic iron or iron oxide (Sofia et al., 2006; Min et al., 2007). The bulk of our presolar grains, therefore, have compositions that are more Fe-rich than those expected from astronomical observations. Among the grains with olivine-like compositions only one grain, 5-7-o1 from QUE 99177, has a composition consistent with forsterite (mg# = 93), and none of the pyroxene-like grains have compositions consistent with enstatite (Table 2). Fig. 8 shows the distribution of compositions for olivine-like and pyroxene-like grains, as well as for those grains with compositions intermediate between these two phases. Overall, the presolar silicates are dominated by grains with compositions that have roughly similar amounts of Fe and Mg or are slightly richer in Fe than Mg (mg#s of 50 or less). However, olivine-like grains are distinctly more Mg-rich than other grains; all but one of the grains have mg#s that are greater than 50. Pyroxene-like grains and grains with intermediate compositions tend to be more Fe-rich; less than half of the intermediate grains and 1/3 of the pyroxene-like grains have mg#s that are greater than 50. The mg#s for Al-rich grains, Si-poor grains, and Si-rich grains are shown in Table 2, but have been omitted from Fig. 8 to avoid clutter. The discovery of abundant Fe-rich presolar grains has been rather unexpected and has been attributed to both primary and secondary processes (Nguyen and Zinner, 2004; Floss et al., 2006; Nguyen et al., 2007); below we discuss these possibilities in more detail.

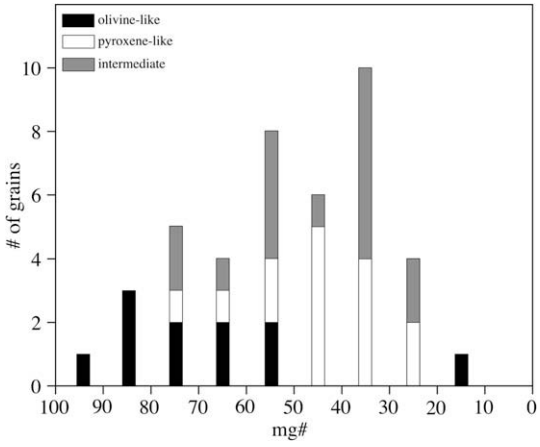

Fig. 8. Histogram showing the Fe–Mg distributions of presolar silicates in QUE 99177 and MET 00426; mg# = Mg/(Mg + Fe) * 100.

The first silicate minerals expected to condense in high temperature O-rich stellar ejecta are essentially pure Mg-endmember forsterite and enstatite (Lodders and Fegley, 1999; Ferrarotti and Gail, 2001; Gail, 2003). If chemical equilibrium is maintained, Fe contents are expected to increase rapidly in these minerals as temperatures decrease below 600K (Lodders and Fegley, 1999; Gail, 2003), providing one possible mechanism for producing Fe-rich olivines and pyroxenes. The difficulty with this scenario is that cation diffusion is so slow at the low temperatures expected in this environment (e.g., Palme and Fegley, 1990; Gail, 2003) that equilibration is essentially prevented in circumstellar shells. An alternative process for enhancing the Fe contents of silicate minerals is through condensation under non-equilibrium conditions. Dust in stellar outflows is, in fact, expected to form in a rapidly cooling environment that is not likely to evolve into an equilibrium state (Gail, 2003) and the fractions of Fe incorporated into olivine and pyroxene during non-equilibrium condensation are considerably higher than those expected for chemical equilibrium (Gail and Sedlmayr, 1999; Ferrarotti and Gail, 2001). Floss et al. (2006) argued for a primary process such as this to account for the high Fe content of a presolar silicate grain from an anhydrous interplanetary dust particle on the grounds that the primitive nature of the IDP effectively ruled out the likelihood that it had experienced significant secondary processing. Experimental studies have also been carried out to understand the condensation of circumstellar dust (e.g., Rietmeijer et al., 1999; Nuth et al., 2000). Such laboratory studies of silicate smokes indicate that kinetic nucleation of Mg, Fe and SiO vapors will produce a variety of Mg or Fe endmember species, but will not produce mixed (Fe, Mg, and Si) oxide grains directly from the vapor. This implies that grains condensing from circumstellar outflows will include MgSiO or FeSiO endmember compositions, but will not include MgFeSiO compositions as primary condensates (Rietmeijer et al., 1999). However, our observations indicate that the vast majority of presolar grains have mixed ferromagnesian compositions that are intermediate between such endmember compositions (Table 2). Moreover, as noted above, Min et al. (2007) suggested that amorphous silicates in general are significantly more Mg-rich than has previously been expected and that Fe is present primarily in phases such as metal and oxide. If these observations are, in fact, correct, then it may be necessary to turn to secondary processes to account for the widespread Fe enrichments seen in presolar silicate grains.

Nguyen and Zinner (2004) initially noted the high Fe contents of the presolar silicates that they found and they,

as well as Nguyen et al. (2007), suggested that contamination from surrounding or underlying Fe-rich matrix silicates could be one possible reason, as many of their identifications were carried out using SEM-EDX. However, the high spatial resolution and surface sensitivity of the Auger Nanoprobe make it more likely that the high Fe contents that we see in the presolar silicates from QUE 99177 and MET 00426 are not just an artifact. Although the backscatter effect in Auger analysis (Stadermann et al., in press) may contribute some Fe signal from surrounding Fe-rich matrix, based on analyses of grains that are known to be Fe-free (e.g., SiC) the amount is limited to at most a few percent and, therefore, cannot account for the large Fe enrichments observed in the presolar silicates from this study. Alternatively, Nguyen and Zinner (2004) suggested that secondary processes may have introduced Fe into presolar silicate grains. Diffusion of Fe during thermal metamorphism (e.g., Jones and Rubie, 1991) can increase the Fe contents of grains that were originally Mg-rich. In principle this process can operate in a nebular environment as well as on meteorite parent bodies. However, formation of Fe-bearing silicates through both solid–solid and gas–solid diffusion under standard solar nebular conditions is unlikely because of the extremely slow diffusion rates (Palme and Fegley, 1990). If such a process took place in the solar nebula, it would likely require an ideal environment such as locally high temperatures or oxidizing conditions. On the other hand, aqueous alteration appears to result in the formation of abundant Fe oxide and hydroxide phases (e.g., Jones and Brearley, 2006), but may not increase the Fe contents of silicate minerals (Abreu and Brearley, 2008). These authors studied the fine-grained materials in GRA 95229, a CR2 chondrite that has undergone only mild aqueous alteration. They found that matrix material in this meteorite had Fe/Si ratios that were intermediate between pristine CR chondrites such as MET 00426 (with a high Fe/Si ratio) and more heavily altered CR chondrites such as Renazzo (with a low Fe/Si ratio); Fe/Si ratios are, moreover, inversely correlated with both Al/Si and Mg/Si ratios. Abreu and Brearley (2008) explained the trend through progressive removal of Fe from the fine-grained silicate material, which is fractionated into magnetite during aqueous alteration, leaving behind Al and Mg in the silicate phases. Thus, while aqueous alteration clearly plays a role in the destruction of presolar silicate grains or the re-equilibration of their oxygen isotopic compositions, as discussed below, it appears not to be responsible for the Fe enrichments seen in the grains.

It is difficult to evaluate the relative roles that primary condensation versus secondary alteration may have played in establishing the Fe contents of our presolar grains. On the one hand, the presolar silicates found in our study are all very small and are surrounded by a matrix that is rich in Fe; even a minor amount of processing might have some effect on the compositions of the grains. Both are also Antarctic meteorites with weathering grades of 'B' and 'Be' for MET 00426 and QUE 99177 respectively (Russell et al., 2002), indicating moderate amounts of rustiness and the presence of evaporite minerals in the latter. The possible effects of terrestrial weathering on the Fe contents of presolar silicate grains are discussed in more detail below. On the other hand, Abreu and Brearley (2006) have shown that QUE 99177 and MET 00426 experienced significantly less secondary processing than other CR chondrites. The matrix material of most CR chondrites is heavily hydrated, containing abundant phyllosilicates (serpentine–saponite intergrowths) as well as magnetite, calcite and sulfides (Krot et al., 2002). In contrast, both QUE 99177 and MET 00426 have low abundances of phyllosilicates (or indeed any crystalline silicates), but instead contain abundant amorphous silicates, indicating that these meteorites may have experienced only partial hydration or that alteration occurred at temperatures too low to cause extensive recrystallization (Abreu and Brearley, 2006). In addition, the carbonaceous matter in QUE 99177 and MET 00426 is quite primitive, with a low degree of crystallinity and detectable concentrations of elements (e.g., N, O, and S) that are typically lost during high-temperature processing (Abreu and Brearley, 2006). These meteorites also appear to be unique among other extraterrestrial materials analyzed to date in that they contain abundant C-anomalous carbonaceous matter of likely interstellar origin (Floss and Stadermann, 2008b). Although such phases have been found in IDPs (Floss et al., 2004, 2006) and in the IOM of other primitive meteorites (Busemann et al., 2006b), the amount of such material in QUE 99177 and MET 00426 (~60–140 ppm; Floss and Stadermann, 2008b) is unprecedented and attests to the primitive nature of these meteorites. Moreover, Martins et al. (2008) found high amino acid contents in these meteorites indicating that their soluble organic matter is also very primitive. Ultimately the only way to determine whether the Fe of our presolar grains are of primary or secondary origin is to measure their Fe isotopic compositions. Unfortunately the small sizes of the grains in this study (Table 1) and the fact that they are embedded in a matrix of Fe-rich material makes it extremely challenging to carry out these measurements with the current capabilities of the NanoSIMS, as Fe isotopes must be measured with an O^- primary beam, which has a significantly lower spatial resolution than the nominal 50-nm Cs^+ primary beam. We note, however, that the only presolar silicate grain measured to date for Fe isotopes did exhibit an anomalous Fe isotopic composition (Mostefaoui and Hoppe, 2004), indicating that the Fe content of this grain was established by primary processes.

4.4. Abundances and distribution of presolar O-anomalous grains

Based on the areas of matrix material analyzed in each meteorite and the surface areas of the grains, we can calculate the abundances of presolar O-anomalous grains in the two CR chondrites to be 220 ± 40 ppm for QUE 99177 and 160 ± 30 for MET 00426 (Fig. 9). These values, which are not corrected for detection efficiencies, are similar to or slightly higher than those observed in the two primitive chondrites, Acfer 094 (145 ± 30 ppm) and ALHA77307 (125 ± 30 ppm) that previously have had the highest observed abundances of presolar silicate/oxide grains (Nguyen et al., 2007). The only extraterrestrial materials which

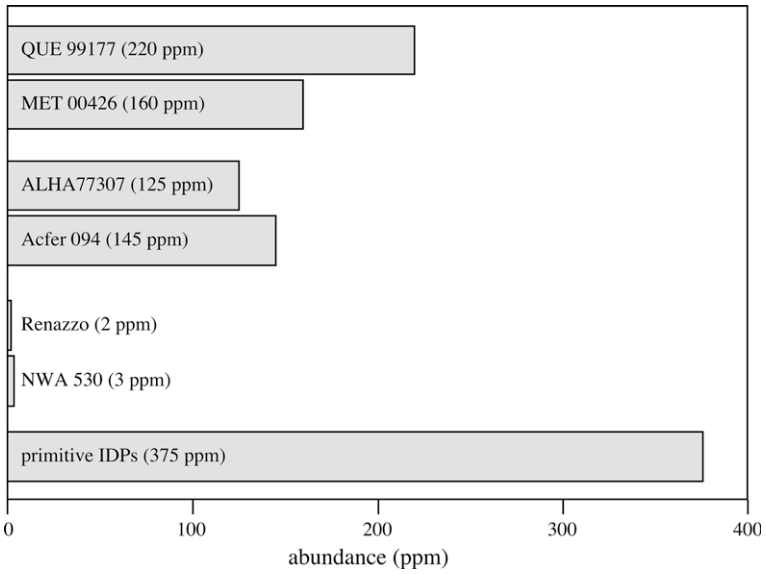

Fig. 9. Bar graph showing the matrix-normalized abundances (ppm) of presolar silicate/oxide grains in various primitive chondrites and IDPs. Data for QUE 99177 and MET 00426 are from this study; other data are from Floss and Stadermann (2005), Floss et al. (2006), Nagashima et al. (2004), and Nguyen et al. (2007).

appear to contain higher abundances of presolar O-anomalous grains are isotopically primitive IDPs, which contain ~375 ppm of presolar silicates (Fig. 9; Floss et al., 2006).

The abundances of presolar O-anomalous grains in QUE 99177 and MET 00426 are significantly higher than previous estimates for other CR chondrites (Fig. 9). Nagashima et al. (2004) found three presolar silicate grains in NWA 530 and calculated an abundance of ~3 ppm for this meteorite. Floss and Stadermann (2005) studied Renazzo and did not find any O-anomalous presolar grains; they estimated an upper limit of ~2 ppm for the abundance of presolar O-anomalous grains in this CR chondrite. These authors suggested that the low abundances of presolar O-anomalous grains in these meteorites could be due to the aqueous alteration they experienced, which might destroy such grains or re-equilibrate their oxygen isotopic compositions. As noted above, Abreu and Brearley (2006) indicated that QUE 99177 and MET 00426 experienced significantly less secondary processing than other CR chondrites and contain amorphous silicates similar to those common in other primitive chondrites that contain abundant presolar grains, such as Acfer 094 and ALHA77307. Thus, it appears likely that the extensive aqueous alteration experienced by CR chondrites is indeed responsible for the lack of presolar silicate/oxide grains in most members of this group. This is also consistent with the low abundance (~3 ppm) of presolar silicate grains found in the CM2 chondrite Murchison, which has experienced extensive aqueous alteration (Nagashima et al., 2005).

There appears to be considerable heterogeneity in the distribution of presolar grains in the matrix material of QUE 99177. From Table 1 it is evident that many more presolar grains were found in matrix areas 5 and 6 than in areas 7 and 8. Calculation of the abundances of presolar grains in matrix areas 5/6 (300 ± 55 ppm; 5400 μm^2 analyzed) and areas 7/8 (90 ± 40 ppm; 3100 μm^2 analyzed) emphasizes these differences. The four areas are all located in the same region of the thin section and, on the scale of an optical microscope or SEM, do not exhibit any obvious petrographic differences that might account for the variable abundances in presolar grains. Moreover, presolar grains are heterogeneously distributed within individual matrix areas and sometimes cluster together. Fig. 10 shows that presolar grains within matrix area 5 of QUE 99177 are more concentrated in some areas than in others. In particular, we found two individual 10×10 μm^2 analysis areas that each contains four presolar grains. More notable, perhaps, is matrix area 5b-10, which contains three different presolar grains in very close proximity. One of the C-anomalous grains is depleted in ^{12}C, whereas the other is enriched; the third grain is a group 1 O-anomalous grain. Thus, the isotopic characteristics of the three grains indicate that they all must have originated from separate presolar sources.

The heterogeneities that we observe in the different matrix areas of QUE 99177 underscore the difficulty inherent in determining accurate estimates of the abundances of presolar grains in different extraterrestrial materials. Indeed, the presolar grain abundance calculated for just matrix area 5 (335 ± 75 ppm; 3400 μm^2 analyzed) is close to the 375-ppm determined for primitive IDPs (Floss et al., 2006). In contrast, the abundance calculated from matrix areas 7/8 is significantly lower and is similar to the abundances determined for ALHA77307 and Acfer 094 (Nguyen et al., 2007). On the other hand, presolar grain abundances in MET 00426 do not show significant differences from one area to another. Thus, matrix areas 5/6 from QUE 99177 may be unusual, with anomalously high abundances of presolar grains. It is possible that this material accreted from a distinct presolar grain-rich reservoir in the solar nebula,

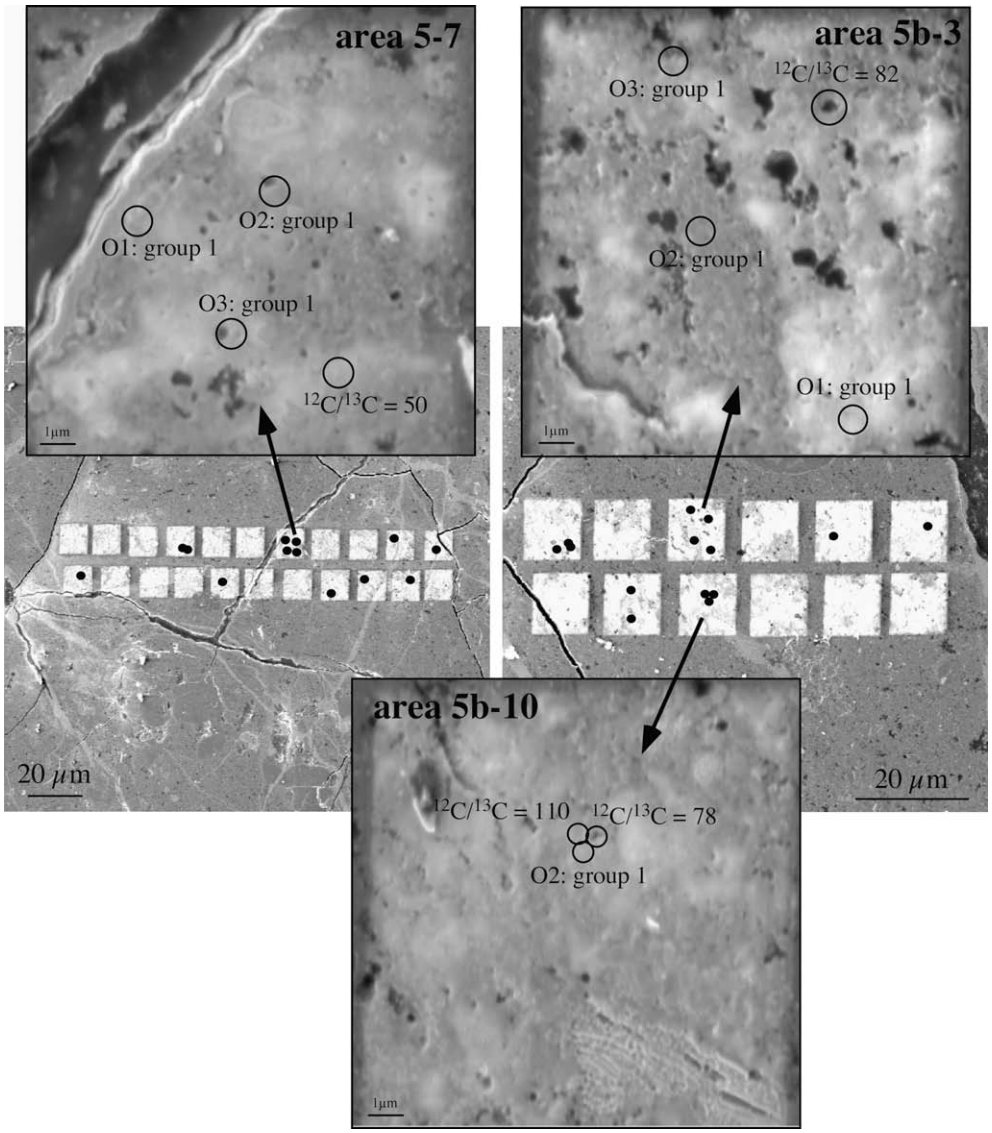

Fig. 10. Field emission secondary electron images showing the distribution of presolar grains in matrix areas of QUE 99177. Each dot represents a presolar grain identified either by its O or C isotopic composition. Areas 5-7 and 5b-3 each contain three O-anomalous group 1 grains as well as a grain with anomalous C isotopic composition. Area 5b-10 contains an O-anomalous group 1 grain and two grains with anomalous C isotopic compositions.

perhaps one similar to that sampled by primitive IDPs, or that it experienced less secondary processing than other matrix regions in QUE 99177. The possible effects of secondary processing on presolar grain abundances are discussed in more detail below.

4.5. Oxide grains in QUE 99177 and MET 00426

The vast majority of the O-anomalous presolar grains found in QUE 99177 and MET 00426 are ferromagnesian silicates and, as noted earlier, we found only one oxide grain among the 54 grains for which we were able to determine elemental compositions. The calculated abundance of oxides in MET 00426 is ~4 ppm and the estimated upper limit for QUE 99177 is on the order of 5 ppm, an order of magnitude lower than previous determinations of the abundances of oxide grains in Acfer 094 and ALHA77307 (30–55 ppm; Nguyen et al., 2007). Nguyen et al. (2008a) recently reported some preliminary data for QUE 99177 in which they report the presence of seven presolar oxide grains among 39 O-anomalous grains located through NanoSIMS isotopic imaging. However, they note that classification of the grains as oxides in solely based on Si to O ion ratios from the NanoSIMS data, and that in the past identification of grains via methods such as Auger spectroscopy (e.g., Nguyen et al., 2008b) has resulted in some grains being reclassified as silicates. Fig. 11 shows the fraction of O-anomalous grains that are oxides in the CR chondrites compared with the primitive meteorites Acfer 094 and ALHA77307. From Fig. 11 it is clear that the relative abundances of presolar oxides are significantly lower in the two CR chondrites than they are in Acfer 094 or ALHA77307,

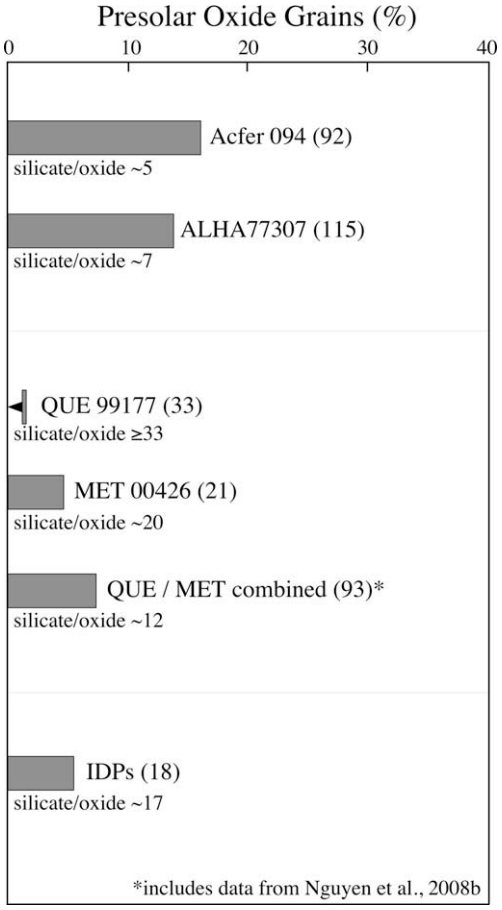

Fig. 11. Bar graph showing the percentages of presolar oxide grains as fractions of the total O-anomalous grains (oxides and silicates) in primitive chondrites and IDPs. The numbers in parentheses after the meteorite names indicate the total number of O-anomalous grains included in the analysis. Also shown are silicate/oxide ratios based on the number of grains of each type found. Data for QUE 99177 and MET 00426 are from this study; other data are from Bose et al. (2007, 2008b), Floss et al. (2006), Messenger et al. (2003a), Messenger et al. (2005), Mostefaoui and Hoppe (2004), Nguyen and Zinner (2004), Nguyen et al. (2007, 2008a,b) and Stadermann et al. (2006).

even when the data of Nguyen et al. (2008a) are included at face value. If we calculate silicate/oxide ratios, we see that Acfer 094 and ALHA77307 have ratios of about 5 and 7, respectively, whereas the ratios for QUE 99177 and MET 00426 are significantly higher, as is the combined silicate/oxide ratio of ~12 obtained if we include the data of Nguyen et al. (2008a). It is interesting to note that IDPs also have low abundances of oxide grains and a high silicate/oxide ratio, with only one Al_2O_3 grain found (Stadermann et al., 2006) versus 17 silicate grains.

It is well-known that secondary processing affects the abundances of presolar grains in different meteorites. For example, Huss and Lewis (1995) have demonstrated that abundances of presolar graphite, SiC and diamond are correlated with petrologic type within different meteorite classes, indicating that thermal metamorphism within the parent bodies destroys the grains. Aqueous alteration also plays an important role in destroying or re-equilibrating the oxygen isotopic compositions of silicate grains, as is evident from the lack of such grains in more heavily altered CR chondrites. In addition, Huss et al. (2003) and Huss (2004) have also invoked pre-accretionary processing of nebular dust, with the preferential destruction of the more labile components, in order to explain differences in the abundances of presolar grains among different meteorite classes; in their model, the CI chondrites and matrix from the CM2 chondrites are the most representative of material inherited from the Sun's parent molecular cloud.

The problem with both the parent body and pre-accretionary alteration scenarios is that it is difficult to envision a process in which oxide grains would be preferentially destroyed over silicate grains. Indeed oxide grains are generally expected to be more resistant to secondary processing than silicate grains (e.g., Nguyen et al., 2007). It is worth considering, however, whether there processes other than thermal or aqueous alteration that could result in the preferential destruction of oxide grains. For example, one possibility might be mechanical erosion. However, it again seems likely that oxide grains would be more resistant to physical destruction than silicate grains. It is also possible that there could have been some type of size sorting in different meteorite classes that would result in the preferential survival or identification of larger grains of one type in a given meteorite group. For example, if silicate grains in Acfer 094 and ALHA77307 were, on average, significantly smaller than oxide grains, they would be harder to detect in imaging searches and would, therefore, be underreported relative to oxide grains. However, if we look at the sizes of presolar silicate and oxide grains found to date in Acfer 094 and ALHA77307 (Mostefaoui and Hoppe, 2004; Nguyen et al., 2007), we find that the range in diameters is almost identical (100–590 μm for oxides and 100–600 μm for silicates) and the median diameters also do not differ substantially (200 μm for oxides and 260 μm for silicates). Silicates in QUE 99177 and MET 00426 have a somewhat more restricted range of diameters (150–390 μm) with a median of 230 μm. The only oxide grain in our study has a diameter of 200 nm. The grains from the two CR chondrites may be slightly smaller than those in Acfer 094 or ALHA77307, but it does not appear that selection effects based on size differences can account for the difference in silicate/oxide ratios between the CR chondrites and the other two primitive meteorites.

If, in fact, oxides are not preferentially destroyed by secondary processing, then the highest silicate/oxide ratios, such as those observed in the CR chondrites and the IDPs, should come closest to reflecting the true initial proportions of presolar silicate and oxide grains in the parent molecular cloud from which the solar nebula evolved. Lower silicate/oxide ratios in meteorites such as Acfer 094 and ALHA77307 could arise in a number of different ways. One possibility, of course, is that the differences are simply the result of insufficient statistics. We have noted above that the distribution of presolar grains is heterogeneous within QUE 99177, an observation that has also been made informally by others for this meteorite and ALHA77307. The matrix areas analyzed in our study may have anomalously

low oxide grain abundances or oxide grain abundances may be unusually high in the measurements of Acfer 094 and ALHA77307. The latter scenario seems less likely, however, given the agreement between the two meteorites and the fact that most of the Acfer 094 data reported in Fig. 11 come from grain size separates whereas the data from ALHA77307 come from thin section measurements. Alternatively, the difference could reflect an intrinsic heterogeneity in the abundances of oxide versus silicate grains in the regions of the solar nebula where different meteorite classes formed. This type of scenario might invoke pre-accretionary processing of the kind envisioned by Huss (2004), in which differential partial vaporization of nebular dust accounts for different abundances of presolar grains in the most primitive members of various meteorite classes. A final possibility is that the differences could be the result of secondary processing, either terrestrially or on the parent bodies of these meteorites. If secondary processing has destroyed silicate grains in Acfer 094 and ALHA77307, this would imply that initial presolar silicate abundances in these meteorites were significantly higher than those currently observed. The first two suggestions can only be verified by additional measurements of these and other meteorites containing abundant presolar grains. Below we discuss in more detail, however, the last possibility, namely that the lower silicate/oxide ratios seen in Acfer 094 and ALHA77307 may be the result of secondary processing.

Both Acfer 094 and ALHA77307 have both long been considered to be among the most primitive of meteorites, with abundant amorphous silicates and little evidence for hydrous or thermal alteration (Brearley, 1993; Greshake, 1997). However, there are some indications that perhaps these meteorites are not as completely unaltered as previously assumed. Acfer 094 is a hot desert meteorite from the Sahara that was originally classified as moderately weathered, with abundant oxide veins (Bischoff and Geiger, 1995), although Greshake (1997) found only minor ferrihydrite and phyllosilicates, indicative of hydrous alteration, in the matrix of Acfer 094. Despite the fact that microRaman observations of the insoluble organic matter (IOM) from this meteorite indicate that it is among the most primitive (Busemann et al., 2007), Alexander et al. (2007) noted that the IOM from Acfer 094 was, in fact, heavily weathered. In addition, Bose et al. (2008b) recently found that presolar silicate grains from Acfer 094 contain a higher fraction of Fe-rich grains than presolar silicates from QUE 99177 and MET 00426. Bland et al. (1998) showed that hot desert weathering resulted in the oxidation of Fe-bearing components in ordinary chondrites, with the proportion of ferric iron directly related to the level of terrestrial weathering. Moreover, they noted a loss of Si and Mg in the most oxidized samples, suggesting that the Fe enhancements seen in the presolar silicates of Acfer 094 could be related to terrestrial weathering. Indeed, Bland et al. (2008) showed that Acfer 094 contained abundant ferric iron, which they attributed to the weathering of amorphous matrix phases. The low silicate/oxide ratio of this meteorite could, therefore, be the result of the terrestrial weathering it has undergone in the Saharan desert, with some silicate grains being destroyed or re-equilibrated during this process. Although the amount of terrestrial aqueous alteration experienced by Acfer 94 appears to have been limited, presolar silicate grains appear to be quite fragile and easily altered. This is evident from the fact that they are only present in low abundances in meteorites as primitive as Semarkona (Tonotani et al., 2006), which is classified as a 3.00 ordinary chondrite (Grossman and Brearley, 2005) and has the most primitive IOM among ordinary chondrites (Busemann et al., 2007).

In contrast to Acfer 094, ALHA77307 from the Antarctic collection appears to be less weathered, with a weathering grade of 'Ae' (Grady, 2000), indicating low levels of rust and the presence of some evaporite minerals. However, although ALHA77307 is the most primitive CO chondrite, the IOM from this meteorite is not as primitive as that from Acfer 094. Raman observations indicate a more ordered character and some potential micrographitization, indicative of a higher degree of thermal metamorphism (Busemann et al., 2007). Moreover, low H/C and N/C ratios and $\delta^{15}N$ and δD values that are close to normal (Alexander et al., 2007) indicate that its IOM is not as primitive as that of the CR chondrites. Thus, some type of secondary processing is suggested by the more ordered nature of the IOM in ALHA77307 and this may also be reflected in the lower silicate/oxide ratio of this meteorite relative to the CRs. The overall abundance of O-anomalous grains is also somewhat lower in ALHA77307 than in the two CR chondrites (125 vs. 160–220 ppm), suggesting a real difference in the degree of processing experienced by the two meteorite groups. As noted above, however, a final determination of the true nebular presolar silicate/oxide ratio will require additional measurements in these and other primitive meteorites.

5. SUMMARY AND CONCLUSIONS

It was long surmised that interplanetary dust particles contained more primitive material than found in the meteorite inventory (e.g., Messenger and Walker, 1997). This assumption has been challenged in recent years by the discovery of large and abundant D and ^{15}N enrichments in extracted insoluble organic matter from primitive chondrites (Busemann et al., 2006a) that rivaled the anomalies previously observed in IDPs (Messenger et al., 2003b), and by observations showing that the most primitive and isotopically anomalous IOM from the CR chondrites and the CM2 chondrite Bells closely resembles that of chondritic porous IDPs (Busemann et al., 2007; Alexander et al., 2007). QUE 99177 and MET 00426 were initially identified as unaltered CR chondrites by Abreu and Brearley (2006), who noted the presence of abundant amorphous silicates and primitive carbonaceous matter. Our study of the stardust inventories of these meteorites has confirmed the primitive nature of these meteorites. Both of these CR chondrites contain high abundances of presolar grains, with concentrations in some regions of QUE 99177 that approach those observed in isotopically primitive IDPs (Floss et al., 2006).

The presolar grain inventories of QUE 99177 and MET 00426 are dominated by ferromagnesian silicates with

group 1 oxygen isotopic compositions, indicative of origins in low mass red giant or AGB stars. Grains with pyroxene-like compositions are somewhat more common than those with olivine-like compositions, but most grains in fact are non-stoichiometric with compositions intermediate between these two phases. This is consistent with recent work suggesting that amorphous interstellar silicates are Mg-rich with a stoichiometry between olivine and pyroxene type silicates (Min et al., 2007). Our presolar grains, however, are much more Fe-rich than predicted by astronomical observations (e.g., Demyk et al., 2000; Min et al., 2007). While secondary alteration may play a role in enhancing the Fe contents of presolar grains, it seems unlikely that the large and ubiquitous Fe enrichments that we observe in this study can be solely due to secondary processing, particularly given the fact that QUE 99177 and MET 00426 appear to be largely unaltered. Stellar outflows are dynamic environments that are not likely to attain equilibrium, and condensation of grains probably proceeds under rapidly changing kinetic conditions that may enhance the likelihood of Fe incorporation over expectations based on equilibrium condensation theory. Ultimately the question of whether the Fe contents of presolar grains were established by primary or secondary processes can only be resolved by measurement of the Fe isotopic compositions of these grains.

Both QUE 99177 and MET 00426 appear to contain unusually low abundances of oxide grains and have elevated silicate/oxide ratios compared to Acfer 094 and ALHA77307. Although this may be a matter of inadequate statistics given the heterogeneous distribution of presolar grains that we have noted, we explore the possibility that secondary processing may have played a role in destroying silicate grains in the latter two meteorites. If silicate grains were preferentially destroyed in Acfer 094 and ALHA77307, this would imply initial presolar silicate abundances at least a factor of two higher than those currently observed for these meteorites.

ACKNOWLEDGMENTS

We thank Tim Smolar for maintenance of the NanoSIMS and Auger Nanoprobe. We appreciate constructive and helpful reviews by Jérôme Aléon and Hugues Leroux. This work was funded by NASA grant NNX07AI82G (PI: C. Floss). Purchase and development of the Auger Nanoprobe was funded by NASA grants NNG06GE18G and NNX08AI13G (PI: F.J. Stadermann).

APPENDIX A. SUPPLEMENTARY DATA

Supplementary data associated with this article can be found, in the online version, at doi:10.1016/j.gca.2009.01.033.

REFERENCES

Abreu N. and Brearley A. (2006) Early solar system processes recorded in the matrices of CR2 chondrites MET 00426 and QUE 99177. *Lunar Planet. Sci. XXXVII*, #2395.

Abreu N. and Brearley A. (2008) Petrologic and chemical effects of the onset of aqueous alteration on the matrices of CR chondrites: GRA 95229. *Lunar Planet. Sci. XXXIX*, #2013.

Aléon J., Robert F., Duprat J. and Derenne S. (2005) Extreme oxygen isotope ratios in the early solar system. *Nature* **437**, 385–388.

Alexander C. M. O'D., Fogel M., Yabuta H. and Cody G. D. (2007) The origin and evolution of chondrites recorded in the elemental and isotopic compositions of their macromolecular organic matter. *Geochim. Cosmochim. Acta* **71**, 4380–4403.

Bischoff A. and Geiger T. (1995) Meteorites from the Sahara: find locations, shock classification, degree of weathering and pairing. *Meteoritics* **30**, 113–122.

Bland P. A., Sexton A. S., Jull A. J. T., Bevan A. W. R., Berry F. J., Thornley D. M., Astin T. R., Britt D. T. and Pillinger C. T. (1998) Climate and rock weathering: a study of terrestrial age dated ordinary chondritic meteorites from hot desert regions. *Geochim. Cosmochim. Acta* **62**, 3169–3184.

Bland P. A., Stadermann F. J., Floss C., Rost D., Vicenzi E., Kearsley A. T. and Benedix G. (2007) A cornucopia of presolar and early solar system materials at the micrometer size range in primitive chondrite matrix. *Meteorit. Planet. Sci.* **42**, 1417–1427.

Bland P. A., Howard K. T., Cressey G. and Benedix G. K. (2008) The terrestrial component of primitive chondrite alteration. *Meteorit. Planet. Sci.* **43**, A26.

Boothroyd A. I. and Sackmann I. J. (1999) The CNO isotopes: deep circulation in red giants and first and second dredge-up. *Astrophys. J.* **510**, 232–250.

Bose M., Floss C. and Stadermann F. J. (2007) Acfer 094 presolar silicates characterized using NanoSIMS and Auger Nanoprobe. *Meteorit. Planet. Sci.* **42**, A23.

Bose M., Stadermann F. J. and Floss C. (2008a) An investigation into the origin of group 4 stardust grains. *Lunar Planet. Sci. XXXIX*, #1099.

Bose M., Floss C. and Stadermann F. J. (2008b) Iron-enriched stardust grains in the meteorites Acfer 094, QUE 99177 and MET 00426. *Meteorit. Planet. Sci.* **43**, A27.

Bradley J. P. (1994) Chemically anomalous preaccretionally irradiated grains in interplanetary dust from comets. *Science* **265**, 925–929.

Bradley J. P. and Dai Z. R. (2004) Mechanism of formation of glass with embedded metal and sulfides. *Astrophys. J.* **617**, 650–655.

Brearley A. (1993) Matrix and fine-grained rims in the unequilibrated CO3 chondrite, ALHA77307: origins and evidence for diverse, primitive nebular dust components. *Geochim. Cosmochim. Acta* **57**, 1521–1550.

Busemann H., Young A. F., Alexander C. M. O'D., Hoppe P., Mukhopadhyay S. and Nittler L. R. (2006a) Interstellar chemistry recorded in organic matter from primitive meteorites. *Science* **312**, 727–730.

Busemann H., Alexander C. M. O'D., Nittler L. R., Zega T. J., Stroud R. M., Cody G., Yabuta H. and Hoppe P. (2006b) Correlated microscale isotope and scanning transmission X-ray analyses of isotopically anomalous organic matter from the CR2 chondrite EET 92042. *Lunar Planet. Sci XXXVII*, #2005.

Busemann H., Alexander C. M. O'D. and Nittler L. R. (2007) Characterization of insoluble organic matter in primitive meteorites by microRaman spectroscopy. *Meteorit. Planet. Sci.* **42**, 1387–1416.

Busso M., Gallino R. and Wasserburg G. J. (1999) Nucleosynthesis in asymptotic giant branch stars: relevance for galactic enrichment and solar system formation. *Ann. Rev. Astron. Astrophys.* **37**, 239–309.

Choi B.-G., Huss G., Wasserburg G. and Gallino R. (1998) Presolar corundum and spinel in ordinary chondrites: origins from AGB stars and a supernova. *Science* **282**, 1284–1289.

Demyk K., Dartois E., Wiesemeyer H., Jones A. P. and d'Hendecourt L. (2000) Structure and chemical composition of the silicate dust around OH/IR stars. *Astron. Astrophys.* **364**, 170–178.

Demyk K., Carrez P., Leroux H., Cordier P., Jones A. P., Borg J., Quirico E., Raynal P.-I. and d'Hendecourt L. (2001) Structural and chemical alteration of crystalline olivine under low energy He^+ irradiation. *Astron. Astrophys.* **368**, L38–L41.

DePew K., Speck A. and Dijkstra C. (2006) Astromineralogy of the 13 μm feature in the spectra of oxygen-rich asymptotic giant branch stars. I. Corundum and spinel. *Astrophys. J.* **640**, 971–981.

Ferrarotti A. S. and Gail H.-P. (2001) Mineral formation in stellar winds. II: Effects of Mg/Si abundance variations on dust composition in AGB stars. *Astron. Astrophys.* **371**, 133–151.

Ferrarotti A. S. and Gail H.-P. (2003) Mineral formation in stellar winds. IV. Formation of magnesiowüstite. *Astron. Astrophys.* **398**, 1029–1039.

Floss C. and Stadermann F. J. (2005) Presolar (circumstellar and interstellar) phases in Renazzo: the effects of parent body processing. *Lunar Planet. Sci. XXXVI*, #1390.

Floss C. and Stadermann F. J. (2008a) The stardust inventories of CR chondrites QUE 99177 and MET 00426, and the distribution of presolar silicate and oxide grains in the early solar system. *Lunar Planet. Sci. XXXIX*, #1280.

Floss C. and Stadermann F. J. (2008b) C-anomalous phases in QUE 99177 and MET 00426. *Meteorit. Planet. Sci.* **43**, A44.

Floss C., Stadermann F. J., Bradley J. P., Dai Z. R., Bajt S. and Graham G. (2004) Carbon and nitrogen isotopic anomalies in an anhydrous interplanetary dust particle. *Science* **303**, 1355–1358.

Floss C., Stadermann F. J., Bradley J. P., Dai Z. R., Bajt S., Graham G. and Lea A. S. (2006) Identification of isotopically primitive interplanetary dust particles: a NanoSIMS isotopic imaging study. *Geochim Cosmochim. Acta* **70**, 2371–2399.

Floss C., Stadermann F. J. and Bose M. (2008) Circumstellar Fe oxide from the Acfer 094 carbonaceous chondrite. *Astrophys. J.* **672**, 1266–1271.

Gail H.-P. (2003) Formation and evolution of minerals. In *Astromineralogy* (ed. T. Henning). Springer-Verlag, Berlin, pp. 55–120.

Gail H.-P. and Sedlmayr E. (1999) Mineral formation in stellar winds. I: Condensation sequence of silicate and iron grains in stationary oxygen rich outflows. *Astron. Astrophys.* **347**, 594–616.

Gourier D., Robert F., Delpoux O., Binet L., Vezin H., Moissette A. and Derenne S. (2008) Extreme deuterium enrichment of organic radicals in the Orgueil meteorite: revisiting the interstellar interpretation. *Geochim. Cosmchim. Acta* **72**, 1914–1923.

Grady M. M. (2000) *Catalogue of Meteorites*. Cambridge University Press, London. 689 pp.

Greshake A. (1997) The primitive matrix components of the unique carbonaceous chondrite Acfer 094: a TEM study. *Geochim. Cosmochim. Acta* **61**, 437–452.

Grossman J. N. and Brearley A. (2005) The onset of metamorphism in ordinary and carbonaceous chondrites. *Meteorit. Planet. Sci* **40**, 87–122.

Huss G. (2004) Implications of isotopic anomalies and presolar grains for the formation of the early solar system. *Antarct. Meteor. Res.* **17**, 132–152.

Huss G. R. and Lewis R. S. (1995) Presolar diamond, SiC, and graphite in primitive chondrites: abundances as a function of meteorite class and petrologic type. *Geochim. Cosmochim. Acta* **59**, 115–160.

Huss G. R., Fahey A. J., Gallino R. and Wasserburg G. J. (1994) Oxygen isotopes in circumstellar Al_2O_3 grains from meteorites and stellar nucleosynthesis. *Astrophys. J.* **430**, L81–L84.

Huss G., Meshik A. P., Smith J. B. and Hohenberg C. (2003) Presolar diamond, silicon carbide, and graphite in carbonaceous chondrites: implications for thermal processing in the solar nebula. *Geochim. Cosmochim. Acta* **67**, 4823–4848.

Jones C. L. and Brearley A. (2006) Experimental aqueous alteration of the Allende meteorite under oxidizing conditions: constraints on asteroidal alteration. *Geochim. Cosmochim. Acta* **70**, 1040–1058.

Jones R. H. and Rubie D. C. (1991) Thermal histories of CO3 chondrites: application of olivine diffusion modelling to parent body metamorphism. *Earth Planet. Sci. Lett.* **106**, 73–86.

Keller L. P. and Messenger S. (2004) On the origin of GEMS. *Lunar Planet. Sci XXXV*, #1985.

Kemper F., Vriend W. J. and Tielens A. G. G. M. (2004) The absence of crystalline silicates in the diffuse interstellar medium. *Astrophys. J.* **609**, 826–837 (Erratum, Astrophys. J. 633, 534).

Kobayashi S., Tonotani A., Sakamoto N., Nagashima K., Krot A. N. and Yurimoto H. (2005) Presolar silicate grains from primitive carbonaceous chondrites Y-81025, ALHA77307, Adelaide and Acfer 094. *Lunar Planet. Sci. XXXVI*, #1931.

Krot A. N., Meibom A., Weisberg M. K. and Keil K. (2002) The CR chondrite clan: implications for early solar system processes. *Meteorit. Planet. Sci.* **37**, 1451–1490.

Lodders K. and Fegley B. (1999) Condensation chemistry of circumstellar grains. In: *Asymptotic Giant Branch Stars* (eds. T. Le Bertre, A. Lebre and C. Waelkens), IAU Symposium No. 191. Astronomical Society of the Pacific, San Francisco, CA, pp. 279–289.

Maldoni M. M., Ireland T. R. and Robinson G. (2008) IRAS 22036 + 5306: an Al_2O_3 oxide-dominated post-AGB star. *Mon. Not. R. Astron. Soc.* **386**, 2290–2296.

Malfait K., Waelkens C., Waters L. B. F. M., Vandenbussche B., Huygen E. and de Graauw M. S. (1998) The spectrum of the young star HD 100546 observed with the Infrared Space Observatory. *Astron. Astrophys.* **332**, L25–L28.

Martins Z., Alexander C. M. O'D., Orzechowska G. E., Elsila J. E., Glavin J. P., Dworkin J. P., Sephton M. A. and Ehrenfreund P. (2008) Amino acid composition of primitive CR2 chondrites. *Meteorit. Planet. Sci.* **43**, A90.

Messenger S. and Walker R. M. (1997) Evidence for molecular cloud material in meteorites and interplanetary dust. In *Astrophysical Implications of the Laboratory Study of Presolar Materials*, vol. 402 (eds. T. J. Bernatowicz and E. Zinner). American Institute of Physics, pp. 545–564.

Messenger S., Keller L. P., Stadermann F. J., Walker R. M. and Zinner E. (2003a) Samples of stars beyond the solar system: silicate grains in interplanetary dust. *Science* **300**, 105–108.

Messenger S., Stadermann F. J., Floss C., Nittler L. R. and Mukhopadhyay S. (2003b) Isotopic signatures of presolar materials in interplanetary dust. *Space Sci. Rev.* **106**, 155–172.

Messenger S., Keller L. P. and Lauretta D. S. (2005) Supernova olivine from cometary dust. *Science* **309**, 737–741.

Min M., Waters L. B. F. M., de Koter A., Hovenier J. W., Keller L. P. and Markwick-Kemper F. (2007) The shape and composition of interstellar silicate grains. *Astron. Astrophys.* **462**, 667–676.

Molster F. J. and Waters L. B. F. M. (2003) Mineralogy of interstellar and circumstellar dust. In *Astromineralogy* (ed. T. Henning). Springer-Verlag, Berlin, pp. 121–170.

Molster F. J., Yamamura I., Waters L. B. F. M., Tielens A. G. G. M., de Graauw T., de Jong T., de Koter A., Malfalt K., van den Ancker M. E., van Winckel H., Voors R. H. M. and Waelkens

C. (1999) Low temperature crystallization of silicate dust in circumstellar disks. *Nature* **401**, 563–565.

Molster F. J., Yamamura I., Waters L. B. F. M., Nyman L.-A., Käufl H.-U., de Jong T. and Loup C. (2001) IRAS 09425–6040: a carbon star surrounded by highly crystalline silicate dust. *Astron. Astrophys.* **366**, 923–929.

Molster F. J., Waters L. B. F. M., Tielens A. G. G. M., Koike C. and Chihara H. (2002a) Crystalline silicate dust around evolved stars. III: A correlation study of crystalline silicate features. *Astron. Astrophys.* **382**, 241–255.

Molster F. J., Waters L. B. F. M. and Tielens A. G. G. M. (2002b) Crystalline silicate dust around evolved stars. II: The crystalline silicate complexes. *Astron. Astrophys.* **382**, 222–240.

Mostefaoui S. and Hoppe P. (2004) Discovery of abundant in situ silicate and spinel grains from red giant stars in a primitive meteorite. *Astrophys. J.* **613**, L149–L152.

Nagahara H. and Ozawa K. (2008) Heterogeneous nucleation and growth of metal on silicates and its astrophysical implication. *Lunar Planet. Sci. XXXIX*, #1241.

Nagashima K., Krot A. N. and Yurimoto H. (2004) Stardust silicates from primitive meteorites. *Nature* **428**, 921–924.

Nagashima K., Sakamoto N. and Yurimoto H. (2005) Destruction of presolar silicates by aqueous alteration observed in Murchison CM2 chondrite. *Lunar Planet. Sci. XXXVI*, #1671.

Nguyen A. N. and Zinner E. (2004) Discovery of ancient silicate stardust in a meteorite. *Science* **303**, 1496–1499.

Nguyen A. N., Stadermann F. J., Zinner E., Stroud R. M., Alexander C. M. O' and Nittler L. R. (2007) Characterization of presolar silicate and oxide grains in primitive carbonaceous chondrites. *Astrophys. J.* **656**, 1223–1240.

Nguyen A. N., Alexander C. M. O' and Nittler L. R. (2008a) An abundant mix of presolar matter in the highly primitive CR chondrite QUE 99177. *Meteorit. Planet. Sci.* **43**, A115.

Nguyen A. N., Stadermann F. J., Nittler L. R. and Alexander C. M. O'D. (2008b) Characterization of presolar silicate and oxide grains using NanoSIMS and Auger spectroscopy. *Lunar Planet. Sci. XXXIX*, #2142.

Nisini B., Codella C., Giannini T. and Richer J. S. (2002) Observations of high-J SiO emission along the HH211 outflow. *Astron. Astrophys.* **395**, L25–L28.

Nittler L. R. (2007) Presolar grain evidence for low-mass supernova injection into the solar nebula. In: *Workshop on the Chronology of Meteorites and the Early Solar System*, pp. 125–126.

Nittler L. R., Alexander C. M. O'D., Gao X., Walker R. M. and Zinner E. K. (1994) Interstellar oxide grains from the Tieschitz ordinary chondrite. *Nature* **370**, 443–446.

Nittler L. R., Alexander C. M. O'D., Gao X., Walker R. M. and Zinner E. (1997) Stellar sapphires: the properties and origins of presolar Al_2O_3 in meteorites. *Astrophys. J.* **483**, 475–495.

Nittler L. R., Alexander C. M. O'D., Gallino R., Hoppe P., Nguyen A. N., Stadermann F. J. and Zinner E. K. (2008) Aluminum-, calcium- and titanium-rich oxide stardust in ordinary chondrite meteorites. *Astrophys. J.* **682**, 1450–1478.

Noguchi T., Ohashi H., Nishida S., Nakamura T., Aoki T., Toh S., Stephan T. and Iwata N. (2008) Discovery of Antarctic micrometeorites containing GEMS and enstatite whiskers. *Meteorit. Planet. Sci.* **43**, A117.

Nollett K. M., Busso M. and Wasserburg G. J. (2003) Cool bottom processes on the thermally pulsing asymptotic giant branch and the isotopic composition of circumstellar dust grains. *Astrophys. J.* **582**, 1036–1058.

Nuth J. A., Hallenbeck S. L. and Rietmeijer F. J. M. (2000) Laboratory studies of silicate smokes: analog studies of circumstellar materials. *J. Geophys. Res.* **105**, 10387–10396.

Palme H. and Fegley B. (1990) High-temperature condensation of iron-rich olivine in the solar nebula. *Earth Planet. Sci. Lett.* **101**, 180–195.

Rauscher T., Heger A., Hoffman R. D. and Woosley S. E. (2002) Nucleosynthesis in massive stars with improved nuclear and stellar physics. *Astrophys. J.* **576**, 323–348.

Remusat L., Palhol F., Robert F., Derenne S. and France-Lanord C. (2006) Enrichment of deuterium in insoluble organic matter from primitive meteorites: a solar system origin? *Earth Planet. Sci. Lett.* **243**, 15–25.

Rietmeijer F. J. M., Nuth J. A. and Karner J. M. (1999) Metastable eutectic condensation in a Mg–Fe–SiO-H_2–O_2 vapor: analogs to circumstellar dust. *Astrophys. J.* **527**, 395–404.

Russell S. S., Zipfel J., Grossman J. N. and Grady M. M. (2002) The Meteoritical Bulletin, No. 86. *Meteorit. Planet. Sci.* **37**, A157–A184.

Sloan G. C., Kraemer K. E., Goebel J. H. and Price S. D. (2003) Guilt by association: the 13 micron dust emission feature and its correlation to other gas and dust features. *Astrophys. J.* **594**, 483–495.

Sofia U. J., Gordon K. D., Clayton G. C., Misselt K., Wolff M. J., Cox N. L. J. and Ehrenfreund P. (2006) Probing the dust responsible for small Magellanic Cloud extinction. *Astrophys. J.* **636**, 753–764.

Sogawa H. and Kozasa T. (1999) On the origin of crystalline silicate in circumstellar envelopes of oxygen-rich asymptotic giant branch stars. *Astrophys. J.* **516**, L33–L36.

Speck A., Barlow M. J., Sylvester R. J. and Hofmeister A. M. (2000) Dust features in the 10-μm infrared spectra of oxygen-rich evolved stars. *Astron. Astrophys.* **146**, 437–464.

Stadermann F. J., Croat T. K., Bernatowicz T., Amari S., Messenger S., Walker R. M. and Zinner E. (2005) Supernova graphite in the NanoSIMS: carbon, oxygen and titanium isotopic compositions of a spherule and its TiC sub-components. *Geochim. Cosmochim. Acta* **69**, 177–188.

Stadermann F. J., Floss C. and Wopenka B. (2006) Circumstellar aluminum oxide and silicon carbide in interplanetary dust particles. *Geochim. Cosmochim. Acta* **70**, 6168–6179.

Stadermann F. J., Floss C., Bose M., and Lea A. S. (in press) The use of Auger spectroscopy for the *in situ* elemental characterization of sub-micrometer presolar grains. *Meteorit. Planet. Sci.*

Stroud R. M., Nguyen A. N., Alexander C. M. O'D., Nittler L. R. and Stadermann F. J. (2008) Transmission electron microscopy of in situ presolar silicates in Allan Hills 77307. *Meteorit. Planet. Sci.* **43**, A148.

Stroud R. M., Floss C. and Stadermann F. J. (2009) Structure, elemental composition and isotopic composition of presolar silicates in MET 00426. *Lunar Planet. Sci. XL*, #1063.

Timmes F. X., Woosley S. E. and Weaver T. A. (1995) Galactic chemical evolution: hydrogen through zinc. *Astrophys. J. Suppl.* **98**, 617–658.

Tonotani A., Kobayashi S., Nagashima K., Sakamoto N., Russell S. S., Itoh S. and Yurimoto H. (2006) Presolar grains from primitive ordinary chondrites. *Lunar Planet. Sci. XXXVII*, #1539.

Toppani A., Libourel G., Robert F. and Ghanbaja J. (2006) Laboratory condensation of refractory dust in protosolar and circumstellar conditions. *Geochim. Cosmchim. Acta* **70**, 5035–5060.

Vollmer C., Hoppe P., Brenker F. E. and Palme H. (2006) A complex presolar grain in Acfer 094—fingerprints of a circumstellar condensation sequence. *Lunar Planet. Sci. XXXVII*, #1284.

Vollmer C., Hoppe P., Brenker F. E. and Holzapfel C. (2007a) Stellar $MgSiO_3$ perovskite: a shock-transformed stardust silicate found in a meteorite. *Astrophys. J.* **666**, L49–L52.

Vollmer C., Hoppe P., Brenker F. and Holzapfel C. (2007b) A presolar silicate trilogy: condensation, coagulation and transformation – new insights from NanoSIMS/TEM investigations. *Lunar Planet. Sci. XXXVIII*, #1262.

Waelkens C., Waters L. B. F. M., de Graauw M. S., Huygen E., Malfait K., Plets H., Vandenbussche B., Beintema D. A., Boxhoorn D. R., Habing H. J., Heras A. M., Kester D. J. M., Lahuis F., Morris P. W., Roelfsema P. R., Salama A., Siebenmorgen R., Trams N. R., van der Bliek N. R., Valentijn E. A. and Wesselius P. R. (1996) SWS observations of young main-sequence stars with dusty circumstellar disks. *Astron. Astrophys.* **315**, L245–L248.

Wasserburg G. J., Boothroyd A. I. and Sackmann I. J. (1995) Deep circulation in red giant stars: a solution to the carbon and oxygen isotope puzzles? *Astrophys. J.* **447**, L37–L40.

Waters L. B. F. M., Molster F. J., de Jong T., Beintema D. A., Waelkens C., Boogert A. C. A., Boxhoorn D. R., de Graauw T., Drapatz S., Feuchtgruber H., Genzel R., Helmich F. P., Heras D. J. M., Huygen R., Izumiura H., Justtanont K., Kester D. J. M., Kunze D., Lahuis F., Lamers H. J. G. L. M., Leech K. J., Loup C., Lutz D., Morris P. W., Price S. D., Roelfsema P. R., Salama A., Schaeidt S. G., Tielens A. G. G. M., Trams N. R., Valentijn E. A., Vandenbussche B., van den Ancker M. E., van Dishoeck E. F., van Winckel H., Wesselius P. R. and Young E. T. (1996) Mineralogy of oxygen-rich dust shells. *Astron. Astrophys.* **315**, L361–L364.

Wilson T. L. and Rood R. T. (1994) Abundances in the interstellar medium. *Ann. Rev. Astron. Astrophys.* **32**, 191–226.

Yada T., Floss C., Stadermann F. J., Zinner E., Nakamura T., Noguchi T. and Lea A. S. (2008) Stardust in Antarctic micrometeorites. *Meteorit. Planet. Sci.* **43**, 1287–1298.

Zinner E. (2004) Presolar grains. In *Meteorites, Planets and Comets*, vol. 1 (ed. A. M. Davis). Elsevier Science, pp. 17–39.

Associate editor: Anders Meibom